THE ASTRONOMICAL JOURNAL VOLUME 106, NUMBER 5 NOVEMBER 1993

THE MULTIPLICITY OF T TAURI STARS IN THE STAR FORMING REGIONS TAURUS–AURIGA AND OPHIUCHUS–SCORPIUS: A 2.2 MICRON SPECKLE IMAGING SURVEY

A. M. GHEZ,[1] G. NEUGEBAUER, AND K. MATTHEWS

Palomar Observatory, California Institute of Technology, Pasadena, California 91125
Electronic mail: aghez@as.arizona.edu, gxn@tacos.caltech.edu, kym@tacos.caltech.edu

Received 1993 March 17; revised 1993 July 28

ABSTRACT

We present the results of a magnitude limited ($K <= 8.5$ mag) speckle imaging survey of 69 T Tauri stars in the star forming regions Taurus–Auriga and Ophiuchus–Scorpius. Thirty-three companion stars were found with separations ranging from 0".07 to 2".5; nine are new detections. This survey reveals a distinction between the classical T Tauri stars (CTTS) and the weak-lined T Tauri stars (WTTS) based on the binary star frequency as a function of separation: *the WTTS binary star distribution is enhanced at the closer separations (< 50 AU) relative to the CTTS binary star distribution.* We suggest that the nearby companion stars shorten the accretion time scale in multiple star systems, thereby accounting for the presence of WTTS that are coeval with many CTTS. The binary star frequency in the projected linear separation range 16 to 252 AU for T Tauri stars (60[±17]%) is a factor of 4 greater than that of the solar-type main-sequence stars (16[±3]%). Given the limited separation range of this survey, the rate at which binaries are detected suggests that *most, if not all, T Tauri stars have companions.* We propose that the observed overabundance of companions of T Tauri stars is an evolutionary effect, in which triple and higher order T Tauri stars are disrupted by close encounters with another star or system of stars.

1. INTRODUCTION

T Tauri stars are a class of young, low mass (0.1 to 3.0 $\mathcal{M}_\odot$), pre-main-sequence stars whose ages are in the range of 10^4–10^7 yr. Most evolutionary theories of how T Tauri stars emerge from the deeply embedded protostellar stage and progress toward the main sequence are based on single star scenarios (e.g., Adams *et al.* 1988); surveys of main-sequence stars, however, have already shown that about 2/3 of the solar-type stars are in multiple star systems (Abt & Levy 1976; Abt 1983; Duquennoy & Mayor 1991). The question therefore arises of how and when these multiple star systems form, for they appear to be the norm as opposed to the exception. The early work of Joy & Van Biesbroeck (1944) showed that 5 of the first 11 known T Tauri stars are binary stars, which suggests that multiple star systems are formed early in the star formation process. Since 1944 more than 450 T Tauri stars have been identified (see, for example, Herbig & Bell 1988), but only recently has the question of how many of these stars are in multiple systems been revisited.

Recent surveys, which have begun to reveal T Tauri companion stars, include lunar occultations (Simon 1992a; Simon *et al.* 1992; Leinert *et al.* 1991; Chen *et al.* 1990; Simon *et al.* 1987), radial velocity measurements (Mathieu 1992a; Mathieu *et al.* 1988), direct imaging work (Simon *et al.* 1992; Zinnecker *et al.* 1992), and speckle imaging work (Leinert *et al.* 1992). Each technique is sensitive to a unique limited range of binary star separations. Thus the different surveys are complementary, since several methods of detection are necessary to deduce the fraction of young stars with companions.

This paper reports the results of a magnitude limited speckle imaging survey of T Tauri stars in the star forming regions Taurus–Auriga (Tau–Aur) and Ophiuchus–Scorpius (Oph–Sco). At the distances of these regions, speckle imaging is capable of detecting companion stars that are separated by less than the predicted circumstellar disk size, ~100 AU (e.g., Beckwith & Sargent 1992). Thus speckle imaging techniques permit the study of both the frequency of companion stars and their effect on a circumstellar disk.

2. SAMPLE

This survey was confined to the two nearest star forming regions observable from the northern hemisphere, Tau–Aur (140 pc, Elias 1978) and Oph–Sco (140 pc for Oph, de Geus & Burton 1991; 160 pc for Sco, de Geus *et al.* 1989). These regions have many similarities; in particular, they are both sites of active low mass star formation. They are, however, quite different in their distributions of molecular gas and stellar densities. Both regions have been extensively studied and a considerably body of literature on their stellar and cloud properties exists (e.g., Lada *et al.* 1992; Herbig & Bell 1988, and references therein).

The compilation of Herbig & Bell (1988) and recent x-ray selected source lists (Bouvier & Appenzeller 1991; Walter *et al.* 1993) were used to identify a total of 143 T Tauri stars in the regions of interest. Following the example of many researchers (e.g., Walter 1986; Strom *et al.*

[1]Present address: Steward Observatory, University of Arizona, Tucson, AZ 85721.

 0004-6256/93/106(5)/2005/19/$0.90

1989), the sample was divided into classical T Tauri stars (CTTS), which have an equivalent width $W(\mathrm{H}\alpha) > 10$ Å, and weak-lined T Tauri stars (WTTS), which have $W(\mathrm{H}\alpha) < 10$ Å (the "naked T Tauri" stars defined by Walter are a subset of the WTTS).

For speckle imaging of T Tauri stars, the optimum bandpass is K (2.2 μm) as a result of three competing effects: (1) the spectral energy distributions of T Tauri stars peak near 1 μm, (2) the coherence time of the atmosphere, and hence the exposure time used in speckle imaging, increases with wavelength as λ,[1,2] and (3) beyond 3 μm thermal noise dominates the readout noise of present infrared arrays. The limiting magnitude of the speckle system at Palomar is $K=8.5$ mag. Thus only stars brighter than this were included, resulting in a final observing list of 95 T Tauri stars (66% of the identified T Tauri stars). Since the K magnitudes of T Tauri stars occasionally vary unpredictably, the most recent available magnitudes were used. Many of the stars in the original sample lacked near-infrared photometry and were therefore excluded from the final observing list although they may have been bright enough to measure.

3. OBSERVATIONS

Over the period 1990 July to 1991 November, 69 of the 95 T Tauri stars were observed at the $f/415$ Cassegrain focus of the Hale 5 m Telescope of Palomar Observatory using the 58×62 pixel InSb array camera in the photometric K band. The pixel scale, determined by observing and reconstructing images of several binaries with well known orbits (McAlister & Hartkopf 1988), was $0''.053\times0''.053$ ($\pm0''.001$). All the 19 T Tauri stars on the final observing list brighter than $K=7.0$ mag were observed; 26 stars with $7.0<K<=8.5$ mag remain to be measured. Table 1(a) lists the 24 stars observed in Oph–Sco along with their positions, K magnitudes, CTTS/WTTS designation, and assumed distances. Likewise, Table 1(b) presents the same information for the 45 stars observed in Tau–Aur.

Table 2 is a journal of the observations. For each source the observations proceeded in a number of object/calibrator "pairs." A "pair" consists of a series of 400 snapshots (100 ms exposures) on the object of interest followed by a similar series of measurements on a calibrator source. Here the "calibrator" is a source expected to be unresolved by the 5 m telescope. Given the unprecedented angular resolution achieved, two calibrator stars were observed for each target star to ensure that at least one calibrator is an unresolved point source. Calibration of the calibrators against one another provided an adequate check that this was true. Both calibrators, if point sources, were used in the initial image reconstruction, but in most cases one calibrator is preferred due to the other being either too bright or significantly farther away from the target. Table 2 lists the calibrator star used in the final data reduction, the number of sets obtained, and the seeing at 2.2 μm. The FWHM of integrated calibrator data provided an estimate of the typical 2.2 μm seeing during these observations, $0''.85\pm0''.23$.

TABLE 1(a). Oph–Sco sample.

HBC	Name	RA (1950)	DEC (1950)	K (mag)	Ref^{K}	Type	Ref^{TTS}	Dist	Ref^{Dist}
254	AS 205	16 08 37.7	-18 30 43	5.8	5	ctts	1	160	8
637	DoAr 21	16 23 01.7	-24 16 50	6.1	4	wtts	2	140	9
649	RNO 90	16 31 17.5	-15 42 04	6.5	6	ctts	1	140	9
639	DoAr 24 E	16 23 22.0	-24 14 14	6.7	4	wtts	2	140	9
	ROXs 43A	16 28 18.1	-24 23 40	6.7	3	wtts	2,3	140	9
270	V1121 Oph	16 46 25.2	-14 16 56	6.8	5	ctts	1	140	9
264	SR 9	16 24 38.9	-24 15 23	6.9	4	ctts	1,2	140	9
262	SR 24 S	16 23 56.6	-24 38 55	7.1	7	ctts	1	140	9
	155203-2338	15 52 02.6	-23 38 29	7.1	3	wtts	3	160	8
643	SR 20	16 25 31.2	-24 16 08	7.1	4	ctts	1,2	140	9
	ROXs 42C	16 28 13.6	-24 27 36	7.2	3	wtts	2,3	140	9
257	Haro 1-4	16 22 10.6	-23 12 26	7.3	4	ctts	1	140	9
268	Haro 1-16	16 28 31.7	-24 21 10	7.5	4	ctts	1,2	140	9
634	160946-1851	16 09 46.4	-18 51 48	7.5	3	wtts	3	160	8
259	SR 4	16 22 54.9	-24 14 02	7.5	4	ctts	1,2	140	9
630	160815-1857	16 08 14.7	-18 57 02	7.7	3	wtts	3	160	8
267	Haro 1-14	16 28 03.9	-23 58 12	7.8	4	ctts	1	140	9
	162218-2420	16 22 18.1	-24 20 01	7.8	3	wtts	3	140	9
266	V853 Oph	16 25 43.7	-24 21 42	8.0	4	ctts	1,2	140	9
	155913-2233	15 59 12.6	-22 33 09	8.1	3	wtts	3	160	8
633	160905-1859	16 09 05.1	-18 59 12	8.1	3	wtts	3	160	8
638	DoAr 24	16 23 15.8	-24 13 36	8.1	4	ctts	1,2	140	9
	155828-2232	15 58 27.8	-22 32 18	8.5	3	wtts	3	160	8
	160827-1813	16 08 27.3	-18 13 11	8.5	3	wtts	3	160	8

HBC = Catalogue entry number in Herbig & Bell (1988)

(1) Herbig & Bell (1988)
(2) Bouvier & Appenzeller (1991)
(3) Walter et al. (1993)
(4) Rydgren et al. (1976)
(5) Glass & Penston (1974)
(6) Herbst & Warner (1981)
(7) Graham (1991)
(8) de Geus et al. (1989)
(9) de Geus & Burton (1991)

TABLE 1(b). Tau–Aur sample.

HBC	Object	RA (1950)	DEC (1950)	K (mag)	Ref^{K}	Type	Ref^{TTS}	Dist	Ref^{Dist}
35	T Tau	04 19 04.2	+19 25 05	5.3	6	ctts	1	140	11
34	RY Tau	04 18 50.8	+28 19 35	5.7	7	ctts	1	140	11
79	SU Aur	04 52 47.8	+30 29 19	6.0	5	wtts	1,14	140	11
74	DR Tau	04 44 13.2	+16 53 24	6.4	3	ctts	1	140	11
367	V773 Tau	04 11 07.3	+28 04 41	6.5	4	wtts	1	140	11
37	DG Tau	04 24 01.0	+25 59 36	6.7	3	ctts	1	140	11
36	DF Tau	04 23 59.6	+25 35 41	6.8	2	ctts	1	140	11
25	CW Tau	04 11 11.3	+28 03 27	6.9	3	ctts	1	140	11
80/81	RW Aur	05 04 37.7	+30 20 14	6.9	2	ctts	1	140	11
380	HDE 283572	04 18 52.5	+28 11 07	6.9	8	wtts	1,14	140	11
404	V807 Tau	04 30 05.2	+24 03 39	6.9	11	ctts	1	140	11
76	UY Aur	04 48 35.7	+30 42 14	7.0	3	ctts	1	140	11
45	DK Tau	04 27 40.5	+25 54 59	7.1	9	ctts	1	140	11
49	HL Tau	04 28 44.4	+18 07 36	7.1	3	ctts	1	140	11
50	XZ Tau	04 28 46.0	+18 07 35	7.2	3	ctts	1	140	11
415	HP Tau/G2	04 32 54.2	+22 48 08	7.3	13	wtts	1,14	140	11
52	UZ Tau E	04 29 39.3	+25 46 13	7.3	9	ctts	1	140	11
374	Hubble 4	04 15 40.9	+28 12 54	7.3	11	wtts	1	140	11
57	GK Tau	04 30 32.8	+24 14 52	7.3	4	ctts	1	140	11
66	HP Tau	04 32 52.8	+22 48 18	7.3	13	ctts	1	140	11
402	FZ Tau	04 29 30.1	+24 13 44	7.5	8	ctts	1	140	11
386	FV Tau	04 23 49.8	+26 00 13	7.5	8	ctts	1	140	11
67	DO Tau	04 35 24.2	+26 04 55	7.5	7	ctts	1	140	11
54	GG Tau	04 29 37.1	+17 25 22	7.5	13	ctts	1	140	11
29	V410 Tau	04 15 24.8	+28 20 02	7.5	4	wtts	1	140	11
396	Haro 6-13	04 29 13.6	+24 22 43	7.6	8	ctts	1	140	11
368	LkCa 3	04 11 42.8	+27 45 05	7.6	12	wtts	12	140	11
56	GI Tau	04 30 32.3	+24 15 03	7.6	4	ctts	1	140	11
33	DE Tau	04 18 49.8	+27 48 05	7.7	7	ctts	1	140	11
55	GH Tau	04 30 04.8	+24 03 18	7.7	3	ctts	1	140	11
61	CI Tau	04 30 52.2	+22 44 17	7.8	7	ctts	1	140	11
423	LkHα 332/G1	04 39 03.4	+25 17 24	7.8	8	wtts	8	140	11
59	IS Tau	04 30 32.7	+26 15 03	8.0	4	ctts	1	140	11
30	DD Tau	04 15 25.1	+28 09 15	8.0	3	ctts	1	140	11
41	IQ Tau	04 26 47.7	+26 00 16	8.0	3	wtts	1,14	140	11
32	BP Tau	04 16 08.6	+28 59 15	8.0	7	ctts	1	140	11
398	V928 Tau	04 29 17.2	+24 16 08	8.0	8	wtts	1	140	11
44	FX Tau	04 27 27.9	+24 20 18	8.1	3	ctts	1	140	11
369	FO Tau	04 11 43.6	+28 05 02	8.1	8	ctts	1	140	11
53	UZ Tau W	04 29 39.3	+25 46 13	8.1	9	ctts	1	140	11
24	FN Tau	04 11 08.6	+28 20 27	8.2	3	ctts	1	140	11
39	DI Tau	04 26 38.0	+26 26 20	8.4	4	wtts	1	140	11
388	042417+1744	04 24 17.2	+17 44 03	8.4	8	wtts	1	140	11
28	CY Tau	04 14 27.7	+28 13 29	8.4	3	ctts	1	140	11
378	V819 Tau	04 16 19.9	+28 19 03	8.5	8	wtts	1	140	11

(1) Herbig & Bell (1988)
(2) Rydgren et al. (1976)
(3) Rydgren & Vrba (1983)
(4) Rydgren & Vrba (1981)
(5) Warner et al. (1977)
(6) Skrutskie (1992)
(7) Rydgren et al. (1982)
(8) Walter et al. (1988)
(9) Cohen & Kuhi (1979)
(10) Simon et al. (1992)
(11) Elias (1978)
(12) Herbig et al. (1986)
(13) Moneti & Zinnecker (1991)
(14) Strom et al. (1989)

4. DATA ANALYSIS AND RESULTS

The data obtained for each of the 69 target stars were analyzed using speckle imaging techniques described by Ghez (1992). Both deconvolution of the ensemble averaged autocorrelation function (ACF) of the target star with that of its calibrator and division of their power spectra offered estimates of the object's Fourier amplitudes. Although in theory these methods are Fourier equivalents, in practice they differ (see Sec. 4.1). The Fourier phases for each target were retrieved by calculating the bispectrum of the object and fitting the bispectrum phases using a global least-squares algorithm. A Fourier inversion of these amplitudes and phases was used to produce a final image (see Fig. 1), although the image was unnecessary for the following analysis.

4.1 Finding Binary Stars and Fitting for their Parameters

Speckle imaging with the 5 m telescope spatially resolved much closer binary systems than previously possible with direct imaging by a factor ~20. Companion stars in the speckle data were initially identified through the CLEAN process of deconvolving the measured object's

ACF with that of its calibrator (see Gorham *et al.* 1990). Secondary sources at least 5σ above the background noise level are classified as companion stars.

Although calibrated ACFs reveal companion stars, calibrated power spectra were used to provide estimates of their flux density ratio (R) and separation ($\mathbf{s}$). The ACF and power spectra are interchangeable, but a systematic readout noise of the detector is most easily identified and eliminated in the power spectrum domain. In both cases, there is a 180° ambiguity in the position angle of the binary systems; this is resolved by inspecting the Fourier phases (or equivalently the resulting image).

Figure 1(a), the calibrated and normalized power spectrum for DD Tau, illustrates the characteristic fringe pattern of a binary star,

$$P(\mathbf{f}) = \frac{R^2+1+2R\cos(2\pi\mathbf{f}\cdot\mathbf{s})}{R^2+1+2R}.$$

For brighter targets, the object's power spectrum dominates (see Ghez *et al.* 1991), but spikes typical of the detector readout noise are clearly visible. The data analysis removed these corrupted areas of the power spectrum by setting minimum and maximum allowed values. A template mask excluded other spatial frequencies that (1) contained aliased power due to the slightly oversized pixels (53 as opposed to 45 mas/pixel), (2) were outside the diffraction limit, or (3) were less than 2 cycles/arcsec, in order to eliminate the most severe effects of seeing miscalibration (Christou *et al.* 1985). A one-dimensional power spectrum along the separation axis of the two stars was then generated by averaging the two-dimensional power spectrum in the direction perpendicular to the separation axis. Fits to this one-dimensional power spectrum provided estimates of the binary system flux density ratio and separation. Figure 2 shows the one-dimensional power spectrum for DD Tau and the corresponding model fit.

Two stars warrant special attention: in the widely separated ($s>2''$) binary, DK Tau, the companion star is detected, but much of its flux fell off the edge of the field of view. The binary star parameters were not well determined from these observations and are not reported here.

Figure 3 shows components of the second case, the triple system RW Tau, labeled A, B, and C in order of decreasing 2.2 μm flux density. The analysis of this system proceeded in two steps, each of which dealt with the inter-

TABLE 2(a). Journal of observations Oph–Sco.

Date	Object	Cal (SAO)	Sets	Seeing at K (")
1990 July 7	AS 205	159745	3	0.9
	RNO 90	159948	4	0.7
	V1121 Oph	160116	4	0.8
1990 July 8	155913-2233	183901	5	0.7
	155203-2338	183901	4	0.7
	162218-2420	183901	4	0.6
	ROXs 42C	184549	5	0.8
	ROXs 43A	184549	4	0.7
1990 July 9	DoAr 21	184429	4	0.9
	SR 24 S	184549	4	0.9
	DoAr 24 E	184549	6	0.9
	SR 9	184549	4	0.9
	SR 20	184549	4	0.9
	Haro 1-16	184549	4	1.2
	Haro 1-4	184549	4	0.9
	SR 4	184549	4	1.0
1990 Aug 5	SR 9	184549	5	0.9
	160946-1851	159745	4	0.9
	160815-1857	159745	4	0.9
	160905-1859	159745	4	0.9
1990 Aug 6	Haro 1-16	184549	5	0.9
	160827-1813	159745	6	1.0
1990 Aug 7	SR 4	184549	8	1.0
	V853 Oph	184549	8	0.8
	DoAr 24	184549	6	1.0
	155828-2232	183901	4	1.4
1991 May 3	ROXs 42C	184549	6	1.2
1992 Feb 18	Haro 1-14	184429	6	1.0

TABLE 2(b). Journal of observations Tau–Aur.

Date	Object	Cal (SAO)	Sets	Seeing at K (")
1990 Oct 2	RY Tau	76461	8	1.0
	DD Tau	76551	8	1.1
	LkHα 332/G1	76727	4	1.2
1990 Oct 3	V773 Tau	76551	8	1.0
1990 Oct 4	CW Tau	76551	8	0.8
	DD Tau	76551	8	0.7
	RY Tau	76461	8	0.7
	LkHα 332/G1	76727	8	0.7
	SU Aur	57454	10	0.6
1990 Nov 9	DG Tau	76613	9	1.3
	DR Tau	93907	8	1.3
	RW Aur	76876	8	0.9
	DF Tau	76613	5	1.0
1990 Nov 10	HDE 283572	76551	3	1.2
	V807 Tau	76613	8	0.9
	UZ Tau E	76613	8	0.9
	UZ Tau W	76613	8	0.9
	UY Aur	57454	8	1.2
	HL Tau	93907	11	1.2
1991 Oct 18	LkCa 3	76461	2	0.6
	FO Tau	76461	5	0.6
	CY Tau	76461	4	0.6
	V819 Tau	76461	6	0.6
	DI Tau	76727	4	0.6
	FX Tau	76727	2	0.6
	042417+1744	93918	5	0.6
1991 Oct 19	FN Tau	76461	6	0.5
	BP Tau	76461	6	0.5
	IQ Tau	76727	4	0.5
	V928 Tau	76727	6	0.6
	IS Tau	76727	6	0.6
	FZ Tau	76727	6	0.6
	Haro 6-13	76727	6	0.5
	GI Tau	76727	6	0.6
	GH Tau	76727	6	0.6
	CI Tau	76727	4	0.5
1991 Oct 20	V410 Tau	76461	6	0.7
	DE Tau	76485	7	1.1
	Hubble 4	76485	6	0.8
	GK Tau	76727	5	0.8
	FV Tau	76613	6	0.7
	GG Tau	93918	6	0.7
	HP Tau	76727	5	0.8
	HP Tau/G2	76727	5	0.8
	DK Tau	76727	5	0.8
	XZ Tau	93874	5	1.0
1991 Nov 18	T Tau	98918	4	1.4
1991 Nov 19	DO Tau	76618	5	0.9

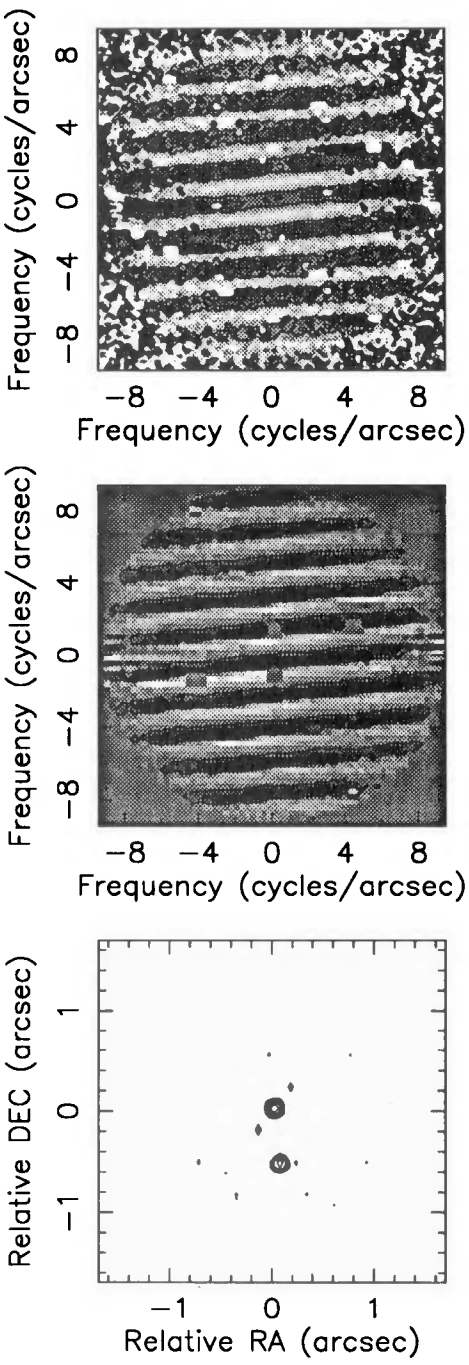

FIG. 1. The reconstruction of the binary star DD Tau from 1990 Oct 4 (a) the calibrated power spectrum (b) the Fourier phases, and (c) the final image.

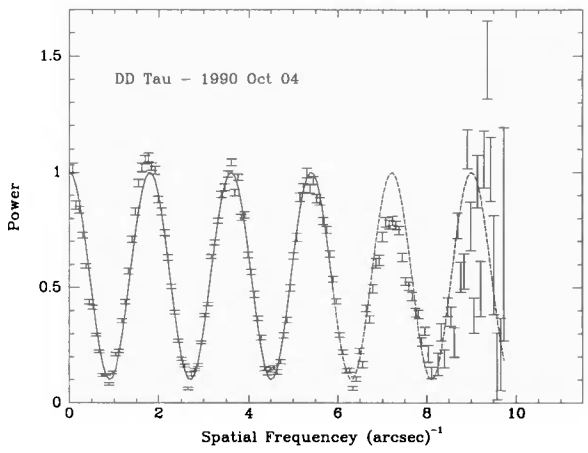

FIG. 2. The one-dimensional power spectrum and model fit for DD Tau. The solid line is over the points that were included in the fit and the dashed line is the extension of the resulting model fit.

ference effects between a set of components. A fit to the lower spatial frequencies of the power spectrum projected along the A–B separation axis provided estimates of the parameters of the wide binary system. This is equivalent to an observation with poorer resolution, which could not resolve component C. The parameters obtained in this first step are for A–(BC) (i.e., the flux density ratio is between star A and the combined light of B and C). Likewise a fit to the power spectrum projection along the B–C separation axis determined the parameters of this close pair.

Among the 69 target objects observed, one triple and 31 binary systems were detected; 9 are new detections. Table 3 lists the fitted binary system parameters and their uncertainties. The relative K band flux of the stars at the time of the observation set their designation as primary, secondary, or tertiary (A, B, and C), where the brightest component is taken as the primary star; the available data did not permit mass estimates for the companion stars. T Tauri stars are known to be variable, so relative brightnesses may well change with time.

The probability that any of the detected double stars are merely chance alignments with a field star is small. Simon *et al.* (1992) estimate that the density of field stars with K magnitudes brighter than 12 mag is $\approx 4\times10^{-5}$ stars/arcsec^2 in the direction of Tau–Aur and $\approx 3\times10^{-4}$ stars/arcsec^2 in the direction of Oph–Sco (Simon 1992b).

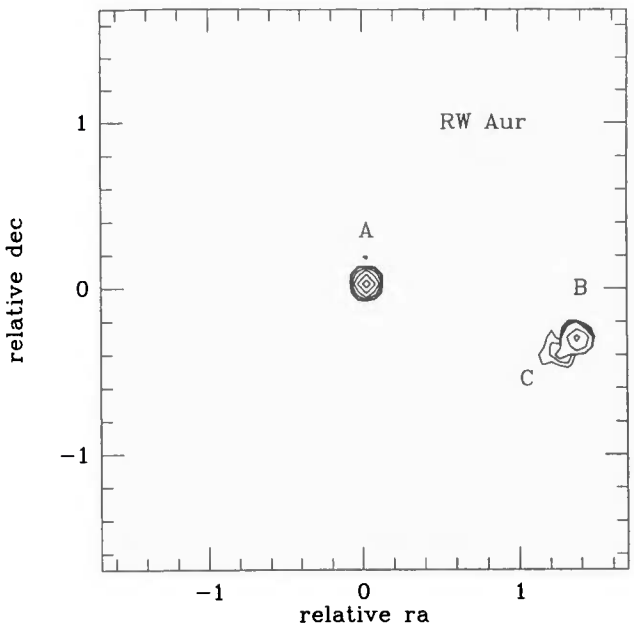

FIG. 3. The speckle image of RW Aur shows a newly discovered third component.

The faintest companion observed has a $K=11$ mag (Fig. 7). As discussed in Sec. 4.2 below, the largest measured binary star separation is $\sim 2''.5$. Of the 45 targets in Tau–Aur, 0.04 are therefore expected to show a field star within a radius of $2''.5$. Likewise, for the 24 targets observed in Oph–Sco, only 0.14 are expected to appear as doubles as a result of a chance projection with a field star.

4.2 Limits for Undetected Companion Stars

The sensitivity of a given observation depends on several factors: (1) the total flux density of the target, (2) the "seeing," or the coherence length (r_0) of the atmosphere, and its stability, (3) the atmospheric coherence time (τ_0) and its stability, (4) the amount of data accumulated on the target, and (5) the systematic electronic readout noise (the strength of which varied from run to run). Each factor has a different effect on the way the sensitivity varies as a function of separation and most of these factors varied from observation to observation. Thus the sensitivity of each observation to finding a companion star as a function of separation is unique. It is essential to evaluate these effects to estimate the completeness of the survey.

In theory, the angular separation range of binary stars detectable by this survey should be constrained only by the diffraction limit of the Hale 5 m Telescope and the field of view of the camera. At $\lambda=2.2$ μm, the diffraction limit corresponds to a maximum spatial frequency, $f_{\max}$, of 11.2 cycles/arcsec. As described earlier the existence of a binary system is revealed in the power spectrum by a sinusoid. Thus the limiting binary star angular separation, $0''.045$, is set by a binary star whose first minimum occurs at $f_{\max}$.

The upper limit for the survey's binary star separation range depends on the camera's field of view. Each target star observed was centered on the array and thus any components outside half the field of view (plus half the seeing disk) were not detected. Since the detector is not circular, the maximum binary star separation that could have been observed depends on the position angle and ranges from $1''.8$ to $2''.5$, where the effects of the array size and the best seeing conditions of $0''.5$ (see Table 2) are considered to give a conservative upper limit. An upper limit of $1''.8$ for the angular separation range eliminates the dependence on position angle.

Within the range of separation of $0''.045$ to $1''.8$, the sensitivity to faint companions is not uniform and increases with increasing separation. In particular, the sensitivity tends to roll off between $0''.1$ and $0''.045$ because the exposure time used (100 ms) did not always match the atmospheric conditions. For example, when the atmospheric coherence time was shorter than the exposure time, the highest spatial frequencies were suppressed.

Limits for *undetected* companion stars at a number of separations can be determined empirically for each observation from the noise level in the power spectrum. The algorithm used was originally suggested by Henry (1991) and is based on the minimum values observed in a group of one-dimensional power spectra made from projections of $P(\mathbf{f})$ at different assumed position angles of an undetected binary star. For each target, 36 one-dimensional power spectra, $p(f)$, are produced by projecting the two-dimensional power spectrum, $P(\mathbf{f})$, at angles between 0° and 175°, with respect to the sky, at 5° intervals. The power spectrum is symmetric and therefore the projections be-

TABLE 3(a). Double star parameters Oph–Sco.

Object	Date	Separation *(arcsec)*	P.A. *(deg)*	Flux Ratio	Notes
SR 20	1990 July 9	0.071 ± 0.001	225 ± 5	8 ± 1	
ROXs 42C	1990 July 8	0.157 ± 0.003	135 ± 3	4.0 ± 0.34	5a
	1991 May 3	0.152 ± 0.003	139 ± 3	4.7 ± 0.3	
160946-1851	1990 Aug 5	0.208 ± 0.004	164 ± 2	3.99 ± 0.06	
162218-2420	1990 July 8	0.236 ± 0.005	156 ± 2	1.25 ± 0.03	4
155913-2233	1990 July 8	0.288 ± 0.005	347 ± 2	2.15 ± 0.03	5a
V853 Oph	1990 Aug 7	0.399 ± 0.008	96 ± 2	4.2 ± 0.5	
SR 9	1990 July 9	0.59 ± 0.01	350 ± 1	11 ± 2	2
	1990 Aug 5	0.59 ± 0.01	350 ± 1	13 ± 2	
Haro 1-4	1990 July 9	0.72 ± 0.01	27 ± 1	4.2 ± 0.2	2
155203-2338	1990 July 8	0.80 ± 0.01	229 ± 1	7.1 ± 0.4	
AS 205	1990 July 7	1.32 ± 0.02	212 ± 1	3.2 ± 0.2	2,3
DoAr 24 E	1990 July 9	2.03 ± 0.04	150 ± 1	5.6 ± 0.9	1

Notes proceeded by an "a" indicate measurements of additional components in these systems that were outside of the separation range of this survey. Otherwise the notes refer to other measurements of the observed binary stars.

(1) Chelli et al. (1988) identified the companion using direct near infrared imaging techniques

(2) Weintraub (1989) detected these binary stars using one-dimensional near-infrared speckle measurements. The discrepancies between these results and the survey presented here are easily accounted for by the limited angular resolution obtained by Weintraub (1989) ($f_{\max}$=0.3–3.6*cycles/arcsec*)

(3) Cohen & Kuhi (1979) identified the secondary component directly at optical wavelengths

(4) Aitken (1939) and Heinz (1980) detected this companion at optical wavelengths with micrometer measurements.

(5a) Mathieu et al. (1988) detected both a spectroscopic binary companion in both 162814-2427 (ROXs 42C)and 155913-2233: thus both systems consist of at least three stars.

TABLE 3(b). Double star parameters Tau–Aur.

Object	Date	Separation (arcsec)	P.A. (deg)	Flux Ratio	Notes
DF Tau	1990 Nov 9	0.088 ± 0.002	329 ± 5	2.13 ± 0.02	1
V773 Tau	1990 Oct 3	0.112 ± 0.002	295 ± 4	2.15 ± 0.01	8
DI Tau	1991 Oct 18	0.12 ± 0.01	294 ± 4	8 ± 1	1
V410 Tau	1991 Oct 20	0.123 ± 0.002	218 ± 4	6.2 ± 0.9	
FO Tau	1991 Oct 18	0.166 ± 0.003	182 ± 3	1.53 ± 0.03	8
V928 Tau	1991 Oct 19	0.165 ± 0.003	125 ± 3	1.66 ± 0.02	8
LkHα 332/G1	1990 Oct 4	0.215 ± 0.004	77 ± 2	1.78 ± 0.02	8
	1990 Oct 2	0.201 ± 0.004	261 ± 2	3.4 ± 0.2	
IS Tau	1991 Oct 19	0.221 ± 0.004	92 ± 2	6.3 ± 0.9	1
GG Tau	1991 Oct 20	0.288 ± 0.006	3 ± 2	4.0 ± 0.1	6,10a
XZ Tau	1991 Oct 20	0.311 ± 0.006	153 ± 2	1.96 ± 0.05	7
GH Tau	1991 Oct 19	0.314 ± 0.006	299 ± 2	1.8 ± 0.02	8
UZ Tau W	1990 Nov 10	0.360 ± 0.007	359 ± 1	2.18 ± 0.07	1
V807 Tau	1990 Nov 9	0.375 ± 0.007	330 ± 1	2.69 ± 0.06	11a,8
LkCa 3	1991 Oct 18	0.491 ± 0.009	77 ± 1	1.046 ± 0.005	8
DD Tau	1990 Oct 4	0.56 ± 0.01	186 ± 1	1.92 ± 0.02	
	1990 Oct 2	0.56 ± 0.01	186 ± 1	2.17 ± 0.07	3,8
T Tau	1991 Nov 18	0.71 ± 0.01	176 ± 1	11 ± 1	4
FV Tau	1991 Oct 20	0.73 ± 0.01	92 ± 1	1.56 ± 0.04	1,6,9a
UY Aur	1990 Nov 10	0.88 ± 0.02	227 ± 1	2.86 ± 0.06	5,2,8
FX Tau	1991 Oct 18	0.90 ± 0.02	291 ± 1	1.965 ± 0.001	
RW Aur A-BC	1990 Nov 9	1.39 ± 0.03	256 ± 1	8 ± 1	5,2,8
RW Aur B-C		0.120 ± 0.004	111 ± 3	41 ± 105	
DK Tau	1991 Oct 20	-	-	-	1,2

Notes proceeded by an "a" indicate measurements of additional components in these systems that were outside of the separation range of this survey. Otherwise the notes refer to other measurements of the observed binary stars.

(1) Simon et al.'s (1992) measured the binary systems DF, DI, FV, and UZ Tau E using lunar occultations and DK Tau using direct imaging techniques. Note: Although IS Tau was initially reported as a single star, the companion was detected in the occultation measurements close to the noise level (Simon 1992b).

(2) Weintraub (1989) detected these binary stars using one-dimensional near-infrared speckle measurements. The discrepancies between these results and the survey presented here are easily accounted for by the limited angular resolution obtained by Weintraub (1989) (f_{max}=0.3–3.6*cycles/arcsec*)

(3) Bouvier et al. (1992) studied this double star at multiple wavelengths using speckle and direct imaging techniques

(4) This double star was first detected by Dyck et al. (1982) with one-dimensional near-infrared speckle interferometry. Ghez et al. (1991) and references within have also studied this double star using high resolution imaging techniques.

(5) Joy & Van Biesbroeck (1944) resolved the widely separated components of RW Aur and UY Aur directly at optical wavelengths.

(6) Leinert et al. (1991) measured the double star GG Tau using one-dimensional speckle imaging techniques and FV Tau using lunar occultations. speckle, and CCD imaging

(7) Haas et al. (1990) measured this double star using one-dimensional near-infrared speckle imaging techniques

(8) Leinert et al. (1992) measure these double stars using near infrared speckle imaging techniques.

(9a) FV Tau appears to consist of at least four stars. FV Tau/c is located 12" away from FV Tau (Herbig & Bell 1988). Both FV Tau (see table) and FV Tau/c have close companions (Simon et al. 1992).

(10a) GG Tau also appears to consist of at least four stars. GG Tau/c is located 10" away from GG Tau (Cohen & Kuhi 1979, Moneti & Zinnecker 1991). Both GG Tau (see table) and GG Tau/c have close companions detected by Leinert et al. (1991).

(11a) Simon (1992b) detected an additional companion with a projected separation of 23 mas from the southern component of the observed binary star V807 Tau (Elias 12). This third component reduces the visibility in our measurements, but no minimum is observed, so the actual separation is between 23 - 45 mas.

tween 180° and 355° offer no new information. As described in Sec. 4.1, certain regions are excluded from these projections.

The minimum values found in the projected power spectra characterize the limit of the flux density ratio (primary/secondary$\geqslant$1) of an undetected binary system. The two-dimensional power spectrum of an unresolved source is completely flat in all directions, $P(\mathbf{f})=1$. For a binary star, $P(\mathbf{f})$ varies sinusoidally along an axis parallel to the binary star separation vector. The amplitude depends on the flux density ratio of the system and the period depends on the magnitude of the binary star separation. The one-dimensional power spectra, $p(f)$, obtained from projections at angles near the separation vector of the binary star should reveal this variation. In contrast, at angles perpendicular to the binary axis, $p(f)$ should be close to unity at all spatial frequencies. The power spectra at the spatial frequency where a first minimum is expected for a

given binary star separation [$f_{1st\ min}=1/(2s)$], sets an upper limit to the flux density ratio for an undetected companion. Minima of the normalized power spectrum translate into flux density ratio limits by the following relationship

$$\text{flux ratio limit}=\frac{1+\sqrt{\text{minimum power}}}{1-\sqrt{\text{minimum power}}}.$$

Since the noise in the power spectrum increases with spatial frequency, limits at many different binary star separations were calculated; Table 4 lists those at 0".1, 0".2, and 0".8. Each projection is normalized by the mean of the projected values at zero frequency [$p(0)$] and the variance of these levels determines the uncertainty quoted for each limit. Figure 4 shows examples of the projected power spectra of sources for which no binary component was seen.

Limits for additional companions can also be obtained for those observations in which multiple systems are detected. The evidence of the observed companions is first removed by expanding the one-dimensional binary star solution to a two-dimensional function and subtracting it from the original data. The residuals are then treated as described above for the single star case. Table 5 contains these limits for additional components in the multiple star systems.

The average limiting flux density ratio for undetected companion stars among the 69 observed targets provides an estimate of the overall survey sensitivity (as opposed to that of the individual observations) for finding faint companion stars. In cases of multiple observations of the same object only the best measurement is included in the average. Figure 5 shows histograms of the limiting flux density ratios at separations of 0".045, 0".055, 0".069, 0".08, 0".1, 0".2, and 0".8, with the mean and the rms value printed in the top right corner of each distribution. The bin farthest to the left in each of the histograms contains observations that have no significant signal at that particular angular resolution, i.e., a $\Delta K=0$ mag binary star would not have been detected.

Figure 6 shows the average limiting sensitivity curve for this survey constructed from the mean values of the distributions in Fig. 5. The circles in Fig. 6 indicate the observed magnitude differences of the detected binary stars. On average, the observations are of sufficient quality to detect binary stars with magnitude differences of up to 3.1 mag for separations between 0".1 and 1".8. Speckle images of individual objects are routinely made with a much higher dynamic range (e.g., Ghez *et al.* 1991; Koresko *et al.* 1991; Henry *et al.* 1992) by obtaining larger data sets. However, a lower overall sensitivity was accepted here in the interest of observing many objects.

Figure 7 shows a different average sensitivity curve evaluated in terms of the limiting K magnitudes for additional companion stars. Its construction follows that of the one shown in Fig. 6 but the flux density ratio limits are combined with the K magnitude of each target found in the literature (Table 1). On average, the observations are sensitive to companion stars brighter than $K=10.6$ mag at distances between 0".1 and 1".8 from the target stars. This is consistent with the estimated apparent magnitudes of the detected companion stars, which are also plotted in Fig. 7.

5. DISCUSSION

5.1 Completeness and Multiplicity

The first few sections of this discussion (Secs. 5.2–5.4) compare the binary star frequencies of various groups of T Tauri stars. To ensure consistency in these comparisons, a subset of the survey is defined as the "complete sample." The first step taken to construct this sample requires each of the included observations, whether or not a companion star was detected, to be sensitive to additional companions within a specified region of the magnitude difference–angular separation phase space. This region, the "completeness region," has been defined to guarantee the detection of all the companion stars with magnitude difference and angular separation within the completeness region for sources in the complex sample. Based on the average sensitivity curve plotted in Fig. 6, the completeness region is restricted to angular separations between 0".1 and 1".8 and magnitude differences between 0.0 and 2.0 mag. Insufficient sensitivity excludes five of the 69 targets observed (155828-2232, 160905-1859, DE Tau, 155913-2233, and DK Tau from the complete sample. Two of the excluded sources are detected as double stars. A second step taken to construct the complete sample converts the angular separation range to a projected linear separation range, since the assumed distances to the star forming regions studied range from 140 to 160 pc (see Column 9 in Table 1). The angular separation range of 0".1 to 1".8 corresponds to projected linear separations of 16 to 288 AU and 14 to 252 AU at the maximum distance of 160 pc and the minimum distance of 140 pc, respectively. Thus the complete sample incorporates only the common range of 16 to 252 AU.

Figure 8 shows the distribution of detected companions for targets in the complete sample. Twenty-two companion stars are included within the completeness region. Outside the boundaries of the completeness region (the outlined area in Fig. 8), the detection of companion stars, such as those of RW Aur, T Tau, and SR 9, is no longer guaranteed. Some observations do show companions outside this region because they have better sensitivity than is required to be a member of the complete sample.

In discussing the data, it is useful to define the true binary star frequency, the ratio of the number of companion stars with any separation and magnitude difference to the number of independent systems a given sample:

$$\text{BSF}=\int_0^\infty \int_0^\infty \frac{d\text{BSF}}{ds\, d\Delta K}\, ds\, d\Delta K.$$

In a specific observational program, the restricted binary star frequency, the bsf, defined as the ratio of companion stars to the number of targets in the completeness region, is measured rather than the BSF. This restricted binary star frequency can be expressed in terms of a differential binary star frequency, $d\text{BSF}/ds\, d\Delta K$,

TABLE 4(a). Limits for stars observed without companion stars in Oph–Sco.

Object	Date	Flux Ratio Limits			Notes
		0."10	0."20	0."80	
V1121 Oph	1990 July 7	47 ± 13	47 ± 13	47 ± 13	
RNO 90	1990 July 7	27 ± 7	27 ± 7	28 ± 8	
SR 24 S	1990 July 9	23 ± 7	23 ± 7	23 ± 7	1a
Haro 1-16	1990 Aug 6	20 ± 4	20 ± 4	20 ± 4	
	1990 July 9	14 ± 3	14 ± 3	14 ± 3	
160815-1857	1990 Aug 5	17 ± 3	18 ± 4	18 ± 4	3a
SR 4	1990 Aug 7	17 ± 4	22 ± 6	23 ± 6	
	1990 July 9	11 ± 2	11 ± 2	11 ± 2	
DoAr 21	1990 July 9	16 ± 2	16 ± 2	16 ± 2	
ROXs 43A	1990 July 8	14 ± 4	14 ± 4	14 ± 4	2a
160827-1813	1990 Aug 6	11 ± 2	11 ± 2	11 ± 2	
DoAr 24	1990 Aug 7	8.0 ± 0.8	15 ± 3	15 ± 3	
Haro 1-14	1992 Feb 18	8 ± 2	8 ± 2	10 ± 3	
160905-1859	1990 Aug 5	3.2 ± 0.3	5.1 ± 0.7	5.4 ± 0.8	
155828-2232	1990 Aug 7	3.0 ± 0.7	3.0 ± 0.7	3.0 ± 0.7	

Notes proceeded by an "a" indicate measurements of additional components in these systems that were outside of the separation range of this survey.

(1a) Haro & Chavira (1974) noted SR 24 to be a wide (6" at P.A. 60°) north - south double star. Simon (1992b) found SR 24 S to be associated with an additional close companion star.

(2a) ROXs 43 appears to consist of at least three stars. Bouvier & Appenzeller (1991) identified the widely separated (6" at P.A. 13°) pair, which they labeled as ROX 43 AB. Mathieu et al. (1988) measured 162819-2423S (ROX 43A) as a spectroscopic binary system.

(3a) Mathieu et al. (1988) discovered a spectroscopic binary in this system.

TABLE 4(b). Limits for stars observed without companion stars in Tau–Aur.

Object	Date	Flux Ratio Limits			Notes
		0."10	0."20	0."80	
DR Tau	1990 Nov 9	43 ± 11	43 ± 11	43 ± 11	
RY Tau	1990 Oct 2	43 ± 12	43 ± 12	45 ± 13	
	1990 Oct 4	27 ± 8	27 ± 8	27 ± 8	
SU Aur	1990 Oct 4	41 ± 14	44 ± 16	44 ± 16	
CW Tau	1990 Oct 4	28 ± 7	34 ± 9	35 ± 10	
BP Tau	1991 Oct 19	26 ± 7	30 ± 10	35 ± 12	
Haro 6-13	1991 Oct 19	25 ± 8	25 ± 8	25 ± 8	
FZ Tau	1991 Oct 19	25 ± 8	25 ± 8	25 ± 8	
DO Tau	1991 Nov 19	24 ± 6	24 ± 6	24 ± 6	
UZ Tau E	1990 Nov 10	22 ± 6	22 ± 6	23 ± 7	
IQ Tau	1991 Oct 19	18 ± 4	18 ± 4	18 ± 4	1a
FN Tau	1991 Oct 19	18 ± 5	18 ± 5	18 ± 5	
HL Tau	1990 Nov 10	16 ± 4	20 ± 6	20 ± 6	
GI Tau	1991 Oct 19	16 ± 6	16 ± 6	16 ± 6	
042417+1744	1991 Oct 18	15 ± 3	16 ± 3	16 ± 3	
DG Tau	1990 Nov 9	14 ± 4	22 ± 7	22 ± 7	
V819 Tau	1991 Oct 18	14 ± 4	14 ± 4	14 ± 4	
CY Tau	1991 Oct 18	14 ± 4	14 ± 4	14 ± 4	
HP Tau	1991 Oct 20	11 ± 2	15 ± 4	16 ± 5	
GK Tau	1991 Oct 20	11 ± 4	11 ± 4	11 ± 4	
CI Tau	1991 Oct 19	10 ± 2	10 ± 2	10 ± 2	
HDE 283572	1990 Nov 10	9 ± 2	9 ± 2	9 ± 2	
HP Tau/G2	1991 Oct 20	9 ± 3	9 ± 3	9 ± 3	2a
Hubble 4	1991 Oct 20	8 ± 2	8 ± 2	8 ± 2	
DE Tau	1991 Oct 20	6 ± 1	8 ± 2	12 ± 4	

Notes proceeded by an "a" indicate measurements of additional components in these systems that were outside of the separation range of this survey.

(1a) Herbig & Bell (1988) detected another star separated by 10" from IQ Tau.

(2a) HP Tau/G2 is located 10" away from HP Tau/G3 (Moneti & Zinnecker 1991)

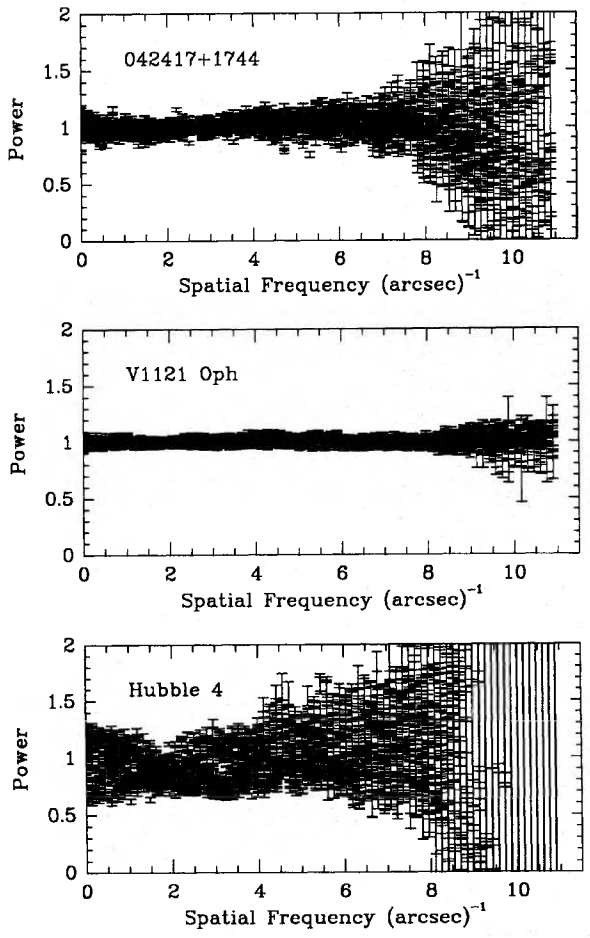

FIG. 4. The 36 one-dimensional power spectra used to place limits on undetected companion stars (see Sec. 4.2) for V1121 Oph, 042417 +1744, and Hubble 4. These three examples show the range of sensitivity obtained in this survey. V1121 Oph is an example of one of the best limits achieved and Hubble 4 is an example of one of the poorest sensitivity observations allowed in the complete sample (see Sec. 5.1).

$$\text{bsf} = \int_{0\text{ mag}}^{2\text{ mag}} \int_{16\text{ AU}}^{252\text{ AU}} \frac{d\text{BSF}}{ds\, d\Delta K}\, ds\, d\Delta K,$$

where s is the projected linear separation, ΔK is the K magnitude difference, and BSF is the total or "true" binary star frequency. Within the completeness region there are 64 targets and 22 companion stars (see Fig. 8); *thus the restricted binary star frequency is 34[± 7]%.*

The target stars with no companions or companions only outside the completeness region are considered as single stars. Therefore the restricted binary star frequency is a lower limit to the true binary star frequency. Nonetheless, the restricted binary star frequency of this sample is well defined and is therefore useful for the comparisons listed in Table 6 and discussed below.

5.2 Binary Stars and Star Forming Regions

One of the goals of this study was to investigate the physical processes that control the formation of multiple star systems. The large fraction of T Tauri stars observed with at least one companion star suggests that multiple stars are formed during the process of star formation, as opposed to being formed at some later time, e.g., by capture (see also discussion below). Thus the various physical and environmental conditions of the regions where these stars originate are presumably among the factors that effect binary star formation. This section examines the multiplicity of T Tauri stars as a function of star forming region, in an attempt to understand what environmental factors affect binary star formation.

The restricted binary star frequency of the complete sample provides the basis for comparing the binary star frequencies of the two star forming regions, Tau–Aur and Oph–Sco. In the completeness region, 6 out of 21 stars in Oph–Sco (29[± 12]%) and 16 out of 43 stars in Tau–Aur (37[± 9]%) have companion stars. Figure 9 shows the

TABLE 5(a). Limits for stars observed as multiple systems in Oph–Sco.

Object	Date	Flux Ratio Limits		
		0."10	0."20	0."80
SR 20	1990 July 9	28 ± 5	30 ± 6	30 ± 6
SR 9	1990 Aug 5	24 ± 7	26 ± 8	27 ± 8
	1990 July 9	16 ± 3	16 ± 3	16 ± 3
ROX 42C	1991 May 3	21 ± 4	23 ± 5	23 ± 5
	1990 July 8	13 ± 4	13 ± 4	13 ± 4
Haro 1-4	1990 July 9	21 ± 4	21 ± 4	24 ± 6
160946-1851	1990 Aug 5	19 ± 3	33 ± 9	33 ± 9
162218-2420	1990 July 8	19 ± 4	20 ± 5	20 ± 5
DoAr 24 E	1990 July 9	19 ± 4	19 ± 4	19 ± 4
155293-2338	1990 July 8	9 ± 2	9 ± 2	12 ± 3
AS 205	1990 July 7	7 ± 1	8 ± 1	8 ± 1
V853 Oph	1990 Aug 7	7 ± 1	7 ± 1	8 ± 2
155913-2233	1990 July 8	5.9 ± 0.8	10 ± 2	12 ± 3

TABLE 5(b). Limits for stars observed as multiple systems in Tau–Aur.

Object	Date	Flux Ratio Limits		
		0."10	0."20	0."80
T Tau	1991 Nov 18	56 ± 18	56 ± 18	56 ± 18
DD Tau	1990 Oct 4	42 ± 10	42 ± 10	42 ± 10
	1990 Oct 2	20 ± 5	21 ± 6	23 ± 7
RW Aur	1990 Nov 9	41 ± 13	41 ± 13	41 ± 13
UY Aur	1990 Nov 10	33 ± 10	36 ± 12	39 ± 14
V807 Tau	1990 Nov 10	25 ± 4	47 ± 13	47 ± 13
FO Tau	1991 Oct 18	23 ± 5	34 ± 9	34 ± 9
UZ Tau W	1990 Nov 10	23 ± 7	23 ± 7	27 ± 10
V928 Tau	1990 Nov 9	20 ± 6	26 ± 9	26 ± 9
DF Tau	1990 Nov 9	20 ± 5	20 ± 5	20 ± 5
DI Tau	1991 Oct 18	17 ± 4	18 ± 5	19 ± 5
LkHα 332/G1	1990 Oct 4	17 ± 3	59 ± 24	59 ± 24
	1990 Oct 2	7 ± 1	12 ± 3	12 ± 3
XZ Tau	1991 Oct 20	15 ± 4	15 ± 4	15 ± 4
IS Tau	1991 Oct 19	13 ± 3	16 ± 4	17 ± 4
GG Tau	1991 Oct 20	12 ± 3	12 ± 3	13 ± 3
FX Tau	1991 Oct 18	12 ± 3	12 ± 3	12 ± 3
V410 Tau	1991 Oct 20	12 ± 3	16 ± 5	16 ± 5
FV Tau	1991 Oct 20	10 ± 2	15 ± 5	16 ± 5
V773 Tau	1990 Oct 3	10 ± 2	10 ± 2	10 ± 2
LkCa 3	1991 Oct 18	9 ± 2	9 ± 2	9 ± 2
GH Tau	1991 Oct 19	7.8 ± 0.8	7.8 ± 0.8	7.8 ± 0.8
DK Tau	1991 Oct 20	5 ± 2	5 ± 2	5 ± 2

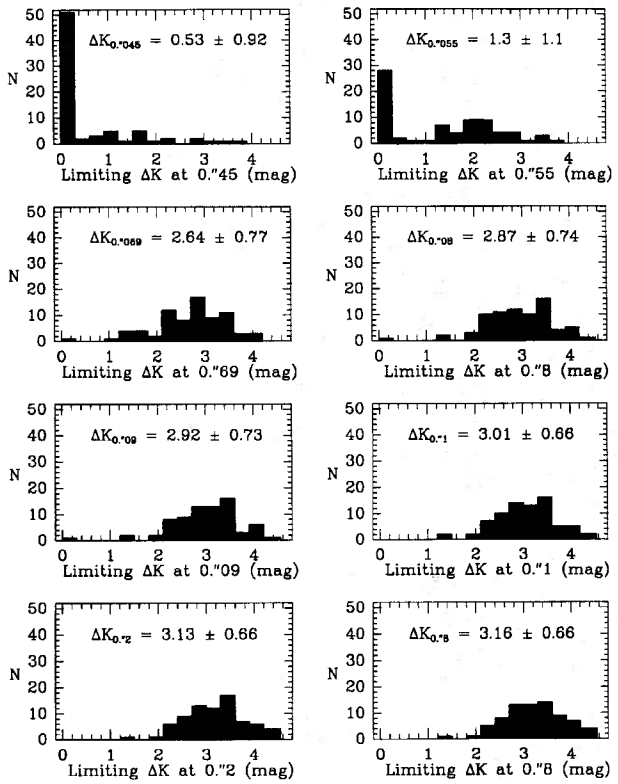

FIG. 5. Histograms of the limiting K magnitude differences for unobserved companions at 0".045, 0".055, 0".069, 0".08, 0".1, 0".2, and 0".8. Each histogram contains a total of 69 limits, one for each target. In the cases of repeated observations of a target star the best limits were used.

restricted binary star frequency for the two regions as a function of separation; they appear to be quite similar. The result of a Kolmogorov–Smirnov test indicates a 0.991 probability that the two distributions are the same as a function of separation between 16 and 252 AU. *Thus there is no statistically significant difference between the binary star frequencies of the two star forming regions over the projected linear separation range 16 to 252 AU.*

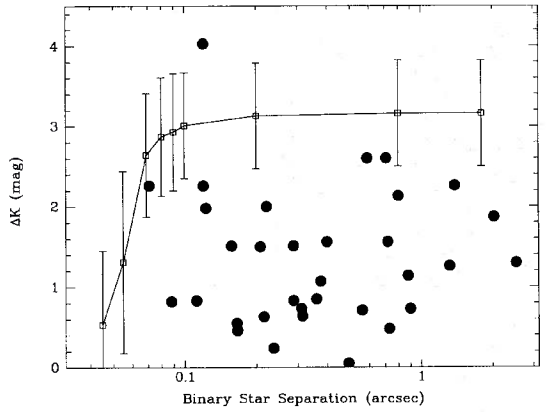

FIG. 6. The average sensitivity curve, measured in terms of limiting K magnitude difference, is plotted as a function of separation. Also plotted here are the observed binary star magnitude differences. *On average* the observations are of sufficient quality to detect binary stars with magnitude difference of up to 3.1 for separations between 0".1 and 1".8.

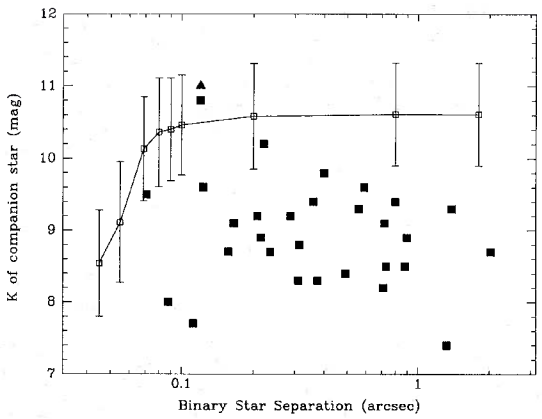

FIG. 7. The average sensitivity curve, measured in terms of limiting apparent K magnitude of a companion star, is plotted as a function of separation. Also plotted here are the observed companion star magnitudes. Secondaries are plotted as squares and the one tertiary is plotted as a triangle. *On average* the observations are of sufficient quality to detect companion stars brighter than $K=10.6$ mag at separations between 0".1 and 1".8.

Tau–Aur and Oph–Sco are alike in that they are both sites of low mass star formation, contain dark clouds (Lynds 1962), and have a total mass of $\approx 10^4 \mathcal{M}_\odot$ (de Geus *et al.* 1990; Ungerechts & Thaddeus 1987). These sites, however, have distinct differences. One distinction between these regions is the presence of a large centrally condensed core and an associated high density of young stellar objects in Oph–Sco. This high mass core (the ρ Oph cloud) appears to have a much higher star forming efficiency (Wilking & Lada 1983; Wilking *et al.* 1989) than the low mass cloud cores which are distributed throughout both regions and are characterized by much lower stellar densities and lower overall star formation efficiency (Myers 1985).

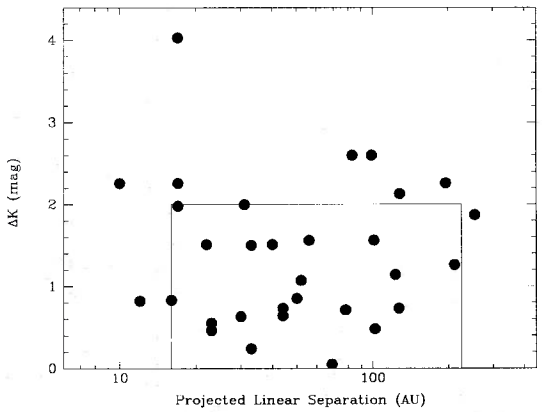

FIG. 8. The distribution of the observed binary stars (circles) and the limits of the completeness region (the outlined area).

TABLE 6. Multiplicity of T Taur stars in the complete sample.[a]

Sample	# Targets	# Companions in completeness region	bsf[b] (%)	Section
Total	64	22	34±7	5.1
Oph–Sco	21	6	29±12	5.2
Tau–Aur	43	16	37±9	
WTTS	22	8	36±13	5.3
CTTS	42	14	33±9	
$\mathcal{M} < 1\mathcal{M}_\odot$	32	13	41±11	5.4
$\mathcal{M} > 1\mathcal{M}_\odot$	32	9	28±9	

[a]The complete sample, discussed in Sec. 5.1, includes all observations sensitive to the "completeness region," i.e., that revealed all companion stars within the projected linear separation range 16 to 252 AU and within the magnitude difference range 0 to 2.0 mag.

[b]The restricted binary star frequency (bsf) incorporates only companion stars within the completeness region, and is therefore a lower limit to the true binary star frequency in the separation range 16 to 252 AU. Nonetheless, it is useful for comparisons of various groups of T Tauri stars, which are discussed in the sections listed in Column 5.

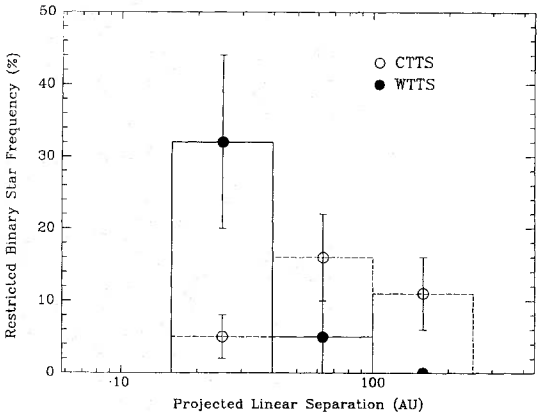

FIG. 10. The binary star frequency as a function of projected linear separation for the WTTS (filled circles) and the CTTS (unfilled circles). The WTTS dominate the binary star distribution at shorter separations whereas the CTTS populate the wider binary star separations.

Lada *et al.* (1992) suggest, on the basis of these differences, that two modes of, or environments for, star formation exist: isolated, i.e., in the scattered low mass cloud cores, and clustered, i.e., in the high mass cloud cores. In the complete sample, the restricted binary star frequency of the ρ Oph cloud core (44[±22]%, 9 stars) is not significantly different from that of Tau–Aur, which is composed of low mass cloud cores.

Five of the T Tauri stars in the Oph–Sco complete sample are members of Sco OB2, an OB association. These stars and those in Oph are thought to be produced from the same giant molecular cloud material (Blaauw 1964; de Geus *et al.* 1989), where the formation of the OB association was triggered at an earlier time then that of the low mass stars in Oph. The restricted binary star frequency of the Sco OB2 sample (40[±28]%) is not statistically different from that of the remainder of the complete sample (34[±8]%). However, neither of these last two comparisons is very sensitive due to the small number of observations in the ρ Oph cloud core and Sco OB2, respectively.

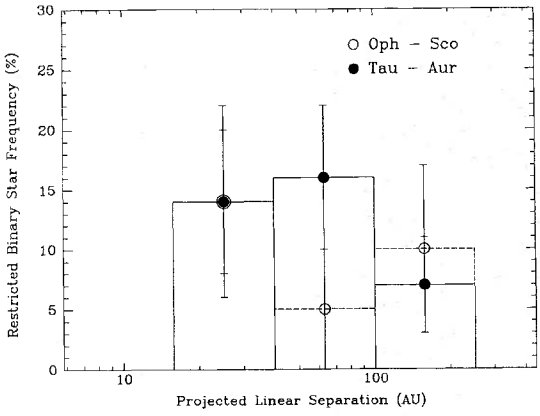

FIG. 9. The binary star frequency as a function of projected linear separation for Tau–Aur (filled circles) and Oph–Sco (unfilled circles). There appears to be no statistically significant difference in the overall binary star frequency between these two star forming regions.

5.3 Binary Stars and Circumstellar Disks

Another aim of this survey was to examine the physical relationship between the two observationally defined subclasses of the T Tauri stars, the classical T Tauri stars (CTTS) and the weak-lined T Tauri stars (WTTS). These two subgroups differ in their Hα emission: CTTS have strong and broad Hα emission [$W(\mathrm{H}\alpha) > 10$ Å] whereas WTTS have weak and narrow Hα emission [$W(\mathrm{H}\alpha) < 10$ Å] (e.g., Herbig & Bell 1988; Strom *et al.* 1989). Most researchers agree that the weak Hα emission observed in WTTS probably originates from the chromosphere, whereas many theories have been presented to account for the presence of strong Hα emission in CTTS. A recent and intriguing proposal suggests that the strong Hα emission arises from disk accretion (Basri & Bertout 1989).

The results of this survey provide an opportunity to investigate the possibility that the underlying difference between the WTTS and the CTTS is related to the presence of a close secondary star. In the completeness region, 14 of the 42 CTTS (33[±9]%) and 8 of the 22 WTTS (36 [±13]%) have companion stars; the binary star frequency appears to be similar in the two subclasses. However, integration over the separation range 16 to 252 AU could have washed out any effect due to circumstellar disks, since such disks are typically assumed to be roughly 100 AU in size. Figure 10 shows the CTTS and WTTS restricted binary star frequency binned as a function of projected linear separation. There is an apparent difference in the dependence on separation; the WTTS populate the binary star distribution at the closer separations and the CTTS dominate the distribution at wider separations. A Kolmogorov–Smirnov test on the data indicates a probability of 0.009 for the two sets being drawn from the same distribution. *Thus*

the distributions of the CTTS and WTTS binary stars as a function of separation are significantly different from each other. The WTTS binary star distribution is enhanced at smaller separations relative to the CTTS binary star distribution.

The observed difference between the CTTS and WTTS binary star distributions suggests that close companion stars play a significant role in the differentiation of these two T Tauri star subclasses. We adopt Basri & Bertout's (1989) model, in which the strong Hα emission of the CTTS arises from the boundary layer of an accretion disk. It has been suggested that all T Tauri stars are formed with an accretion disk (e.g., Shu *et al.* 1987) and therefore would be initially classified as CTTS; they would be observed as WTTS only when their accretion disks are depleted. Walter *et al.* (1988) conclude that the two subclasses are more or less coeval, which suggests that the timescale for disk dispersal depends on more than just the age or mass of the parent T Tauri star. It should be noted, however, that the very oldest population of T Tauri stars appears as WTTS (Walter *et al.*).

A close secondary star can create a gap in the circumstellar disk (Lin & Papaloizou 1992), truncating the amount of material available for accretion. We propose that by reducing the amount of material that can be accreted, the effect of a close secondary star is to shorten the accretion time scale in close binary T Tauri stars. In this way those T Tauri stars with close companions would quickly deplete their accretion disks and appear as WTTS at a fairly early age. Presumably, secondary stars outside the circumstellar disk ($> \sim 100$ AU) should be of no consequence to the accretion time scale.

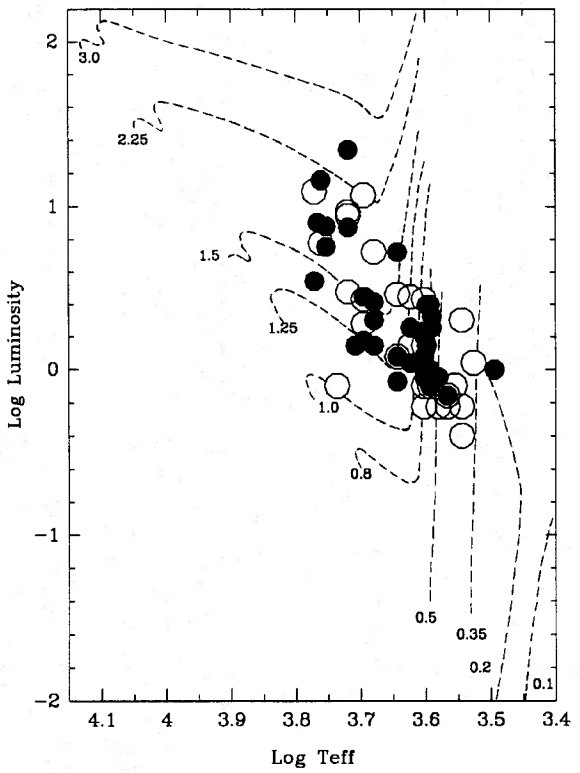

FIG. 11. HR diagram for the stars in the sample. Also plotted are the evolutionary tracks from Cohen & Kuhi (1979). The filled circles are stars observed without companion stars. The unfilled points are those stars observed with companions (the estimated contribution from the companion stars has been removed from the luminosity of these stars).

5.4 Binary Stars and Mass

In theory, T Tauri stars evolve to the main sequence along convective-radiative tracks for low mass stars ($\mathcal{M} < 3.0 \mathcal{M}_\odot$) such as those given by Cohen & Kuhi (1979) and reproduced in Fig. 11. Since the evolutionary tracks for low mass stars are fairly constant in effective temperature, much can be learned just from the spectral types of the stars. Table 7 lists the spectral types of the T Tauri stars in the complete sample and Fig. 12(a) displays their distribution with spectral type. The restricted binary star frequency, shown in Fig. 12(b), suggests a dependence on spectral type. Since the later spectral types in general correspond to lower masses, there may be a dependence on mass.

Mass estimates for these stars can be obtained from their location in the HR diagram with respect to the evolutionary tracks. This requires both the effective temperature, $T_{\rm eff}$, and stellar luminosity, L, for each star. The effective temperatures were derived from the spectral types using the conversion adopted by Cohen & Kuhi (1979). Column 6 of Table 7 lists the stellar luminosities estimated from optical and near-infrared data. These values are used directly for the target stars observed without companion stars. For those stars observed with companions, these luminosities are overestimates due to the extra flux from the secondary stars. The brightest component observed at K is assumed to be the optically identified T Tauri star, for which the spectral type is known, and the measured K flux density ratio is used to divide the previously derived stellar luminosity between the components of the system.

Figure 11 shows the stars in the complete sample in an HR diagram along with the evolutionary tracks from Cohen & Kuhi (1979). The estimated masses for these T Tauri stars range from 0.2 to 2.3 $\mathcal{M}_\odot$ and the distribution peaks between 0.5 and 1.5$\mathcal{M}_\odot$. Figure 13 demonstrates the mass dependence on effective temperature, or equivalently spectral type. By separately grouping spectral types M5 through K7 and K6 through G0, the restricted binary star frequency for T Tauri stars with $\leqslant 1 \mathcal{M}_\odot$ can be compared to that of stars with masses $\geqslant 1 \mathcal{M}_\odot$. In the completeness region, 13 of 32 stars with $\mathcal{M} < \mathcal{M}_\odot$ (41[$\pm$11]%) and 9 of 32 stars with $\mathcal{M} \geqslant 1 \mathcal{M}_\odot$ (28[$\pm$9]%) have companion stars. Although the lower mass stars in the sample have a higher restricted binary star frequency, the difference is not statistically significant. Furthermore, care must be taken in comparing the restricted binary star frequencies of different mass stars. Given the shape of the convective-radiative tracks and the isochrones, magnitude differences most likely reflect mass differences. If the lower mass stars do indeed have a higher restricted binary star frequency, that

would most likely indicate that the lower mass have more high mass ratio (i.e., $\mathcal{M}_1/\mathcal{M}_2$ tends toward one) binary systems than the higher mass targets. Such a distinction would provide a strong constraint on star formation mechanisms.

5.5 T Tauri Versus Main Sequence Binary Stars

The results of this survey indicate that a large fraction of T Tauri stars have companion stars. The youth of these stars ($< \sim 10^7$ yr) suggests that multiple star systems are produced during the early stages of star formation.

To compare the binary star frequency of the T Tauri stars to that of the main-sequence stars, multiplicity surveys of main-sequence stars that have a mass range similar to that of the T Tauri stars were selected. Duquennoy & Mayor (1991) surveyed a sample of nearby solar type main-sequence stars with spectral types F7 to G9. This corresponds to a range in main-sequence masses of $\sim$0.8 to $1.3\mathcal{M}_\odot$. Therefore this sample of main-sequence stars appears to be an appropriate older counterpart for a large percentage (44%) of the T Tauri sample. Fischer & Marcy (1992) investigated the multiplicity of the nearby main-sequence M dwarfs which have masses between $\sim$0.1 and $\sim 0.5\mathcal{M}_\odot$. This mass range incorporates 28% of the T Tauri stars in the complete sample and therefore Fischer and Marcy's study is also useful for comparison with the T Tauri results.

The main-sequence surveys mentioned above combine the results of many detection techniques and therefore cover a much larger binary star separation range than the speckle imaging survey of T Tauri stars. Consequently a comparison between these samples requires a calculation of the binary star frequency for the main-sequence surveys in the projected linear separation range 16 to 252 AU; see Appendix 1.

Since the M dwarf and solar type (F7 to G9) main-sequence stars have similar binary star frequencies in the projected linear separation range 16 to 252 AU, 12[±4]% and 16[±3]%, respectively, and the solar-type main-sequence stars are the older counterparts to the majority of the T Tauri stars, the latter is used for comparison with the T Tauri binary star frequency.

The main-sequence results are corrected for detection biases and therefore provide estimates of the main-sequence binary star frequency integrated over all magnitude differences. Thus the estimate of the binary star frequency in the projected linear separation range 16 to 252

TABLE 7(a). Stars in the complete sample observed without companion stars.

HBC	Name	SpT	Ref	log T_{eff} (K)	L_* (L_O)	Ref	Mass (M_O)
259	SR 4	K6	2	3.623	1.8	2	1.25
262	SR 24 S	K2	1	3.695	2.8	1	1.5
267	Haro 1-14	M0	1	3.593	1.0	1	0.8
268	Haro 1-16	K3	1	3.679	1.4	2	1.25
270	V1121 Oph	K5	1	3.643	5.3	1	1.6
637	DoAr 21	K0	2	3.719	22.0	2	2.5
638	DoAr 24	K5	2	3.643	1.2	2	1.25
649	RNO 90	G5	6	3.753	5.7	16	1.6
	160815-1857	K2	17	3.695	1.5	17	1.3
	160827-1813	K5	17	3.643	0.8	17	1.2
	ROXs 43A	G0	2	3.771	3.5	2	1.35
24	FN Tau	M5	1	3.494	1.0	8	0.2
25	CW Tau	K3	1	3.679	2.6	8	1.55
28	CY Tau	M1	1	3.566	0.7	8	0.45
32	BP Tau	K7	1	3.602	1.2	8	0.8
34	RY Tau	K0	3	3.719	7.5	8	1.9
37	DG Tau	K7	3	3.602	1.7	8	0.8
41	IQ Tau	M0.5	1	3.580	0.9	8	0.5
49	HL Tau	K7	3	3.602	0.9	8	0.8
52	UZ Tau E	M0	3	3.593	0.8	13	0.7
56	GI Tau	K7	1	3.602	1.1	7	0.8
57	GK Tau	K7	1	3.602	1.6	8	0.8
61	CI Tau	K6	3	3.623	1.1	7	1.1
66	HP Tau	K3	1	3.679	2.0	8	1.4
67	DO Tau	K7-M0	1	3.598	1.4	8	0.75
74	DR Tau	M0	3	3.593	2.5	8	0.75
79	SU Aur	G2	3	3.761	14.4	8	2.15
374	Hubble 4	K7-M0	1	3.598	2.5	16	0.8
378	V819 Tau	K7	10	3.602	1.0	8	0.8
380	HDE 283572	G5	10	3.753	7.6	13	1.8
388	042417+1744	K1	10	3.708	1.4	13	1.25
396	Haro 6-13	Cont	1	3.590	2.1	8	0.7
402	FZ Tau	Cont	1	3.590	1.8	14	0.7
415	HP Tau/G2	G1	1	3.766	8.0	13	1.8

References contained in notes following Table 7b.

TABLE 7(b). Stars in the complete sample observed with companion stars.

HBC	Name	SpT	Ref	log T_{eff} (K)	L_*^{old} (L_O)	Ref	L_*^{prim} (L_O)	Mass (M_O)
254	AS 205*	K2	3	3.695	15.3	1	11.7	2.25
257	Haro 1-4*	K6	1	3.623	3.5	1	2.8	1.25
264	SR 9	K7	1	3.602	0.9	2	0.8	0.85
266	V853 Oph*	M1.5	1	3.555	1.0	1	0.8	0.45
639	DoAr 24 E	K0	2	3.719	11.0	2	9.3	2.0
643	SR 20	G0	2	3.771	13.9	2	12.3	2.0
	155203-2338	G2	17	3.761	6.8	17	6.0	1.8
	160946-1851*	K0	17	3.719	3.8	17	3.0	1.5
	162218-2420*	G8	5	3.736	1.5	16	0.8	1.0
	ROXs 42C*	K6	2	3.623	1.8	2	1.4	1.25
29	V410 Tau*	K2	3	3.695	2.2	8	1.9	1.35
30	DD Tau*	M1	1	3.566	1.0	8	0.7	0.45
35	T Tau	K0	3	3.719	8.8	15	8.8	2.0
36	DF Tau	M2	3	3.544	3.0	8	2.0	0.4
39	DI Tau	M0	1	3.593	0.9	8	0.8	0.7
44	FX Tau*	M1	1	3.566	1.0	8	0.7	0.45
50	XZ Tau*	M3	1	3.526	1.6	8	1.1	0.35
53	UZ Tau W*	M2	3	3.544	0.6	14	0.4	0.4
54	GG Tau*	K7	3	3.602	1.8	7	1.4	0.8
55	GH Tau*	M2	1	3.544	0.9	8	0.6	0.4
59	IS Tau*	K2	1	3.695	3.1	8	2.7	1.5
76	UY Aur*	K7	3	3.602	0.8	7	0.6	0.75
80	RW Aur	K5	3	3.623	3.3	14	2.9	1.4
367	V773 Tau*	K3	9	3.679	7.7	8	5.3	1.8
368	LkCa 3*	M1	11	3.566	1.3	12	0.7	0.45
369	FO Tau*	M2	1	3.544	1.0	14	0.6	0.4
386	FV Tau*	K5	1	3.643	2.0	14	1.2	1.0
398	V928 Tau*	M0.5	1	3.580	1.0	1	0.6	0.5
404	V807 Tau*	K7	4	3.602	3.7	16	2.7	0.8
423	LkHα 332/G1*	M1	1	3.566	0.9	14	0.6	0.45

Notes: (*) denotes binary stars that fall within the completeness region, i.e., have separations in the range 16 to 252 AU and magnitudes differences between 0.0 and 2.0 mag.

References for Column 4 (Spectral Type) and Column 7 (Stellar Luminosity). Also noted are the assumed distances to the star forming regions used in the references, which derive stellar luminosities. The stellar luminosities listed in Column 6 have been shifted, when necessary for the distances assumed in this work ($d_{Tau-Aur}$ = 140 pc, d_{Oph} = 140 pc, and d_{Sco} = 160pc).

(1) Cohen & Kuhi (1979); d_{Tau} = 160 pc; d_{Oph} = 170 pc
(2) Bouvier & Appenzeller (1991); d_{Oph} = 170 pc
(3) Basri & Batalha (1990)
(4) Herbig & Bell (1988)
(5) Montmerle et al. (1983)
(6) Herbst & Warner (1981)
(7) Hartigan et al. (1991); d_{Tau} = 160 pc
(8) Beckwith et al. (1990); d_{Tau} = 140 pc
(9) Herbig (1977)
(10) Walter et al. (1988)
(11) Herbig et al. (1986)
(12) Cabrit et al. (1990); d_{Tau} = 160 pc
(13) Strom et al. (1989); d_{Tau} = 160 pc
(14) Cohen et al. (1989); d_{Tau} = 160 pc
(15) Ghez et al. (1991); d_{Tau} = 140 pc
(16) Simon et al. (1992)
(17) Walter et al. (1993)

AU for the T Tauri stars must include all magnitude differences,

$$\mathrm{BSF}' = \int_0^{\infty} \int_{16}^{252} \frac{d\mathrm{BSF}}{ds\, d\Delta K}\, ds\, d\Delta K.$$

An estimate of BSF′ requires a calculation of the distribution, in ΔK, of the binary star frequency for $\Delta K > 2.0$ mag (bsf already accounts for $\Delta K \leqslant 2.0$ mag). This was accomplished by examining strips in the ΔK-projected linear separation parameter space above $\Delta K = 2.0$ mag. For each ΔK strip, spanning 16 to 252 AU and an interval of 0.5 mag in magnitude difference, the number of observations sensitive to this region and, of these, how many have companion stars that fall within that region were determined (see Table 8). There are observations sensitive to magnitude differences of 4.0 mag; beyond this range there is no way of estimating the binary star frequency. Given these uncertainties, the estimated binary star frequency, as derived from these results in the projected linear separation range 16 to 252 AU is 59[±17]%.

In both the main sequence and the T Tauri study the total number of target stars in each was used to normalize the binary star frequency. However, Duquennoy & Mayor's (1991) definition of a target star differs from the one used in this study in the question of how far another star could be before it is considered to be a separate target star. For this discussion the lowest value, 2×10^3 AU, suggested by Duquennoy and Mayor for the cutoff separation is adopted. This affects only the treatment of UZ Tau E and W, which counted previously as two targets and are now

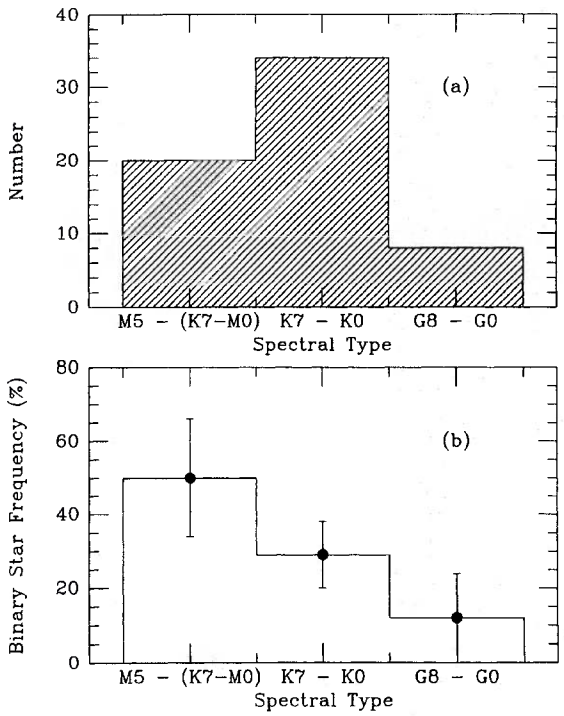

FIG. 12. (a) The distribution of spectral types for the complete sample. (b) The restricted binary star frequency as a function of spectral type.

viewed as one system. This only slightly changes the value for the T Tauri binary star frequency in the projected linear separation range 16 to 252 AU, which was previously estimated to 59[±17]% and is now taken to be 60[±17]%.

The T Tauri binary star frequency appears to be greater than that of the main-sequence stars by a factor of 4 [see Fig. 14(b)]. The discrepancy between the two binary star frequencies is a 2.5σ effect.

The discrepancy between the two binary star frequencies could be due to a difference in the sensitivity of the two surveys, which would imply that this survey is much more

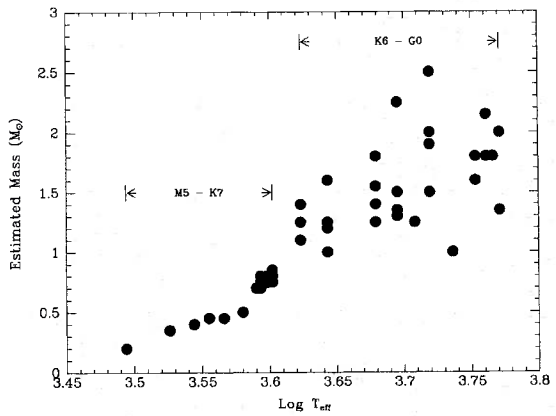

FIG. 13. The estimated mass as a function of effective temperature (or equivalently spectral type).

TABLE 8. T Tauri binary stars frequency.

ΔK Range (mag)	# Obs	# Companions	Freq (%)
0.0 - 2.0	64	22	34 ± 7
2.0 - 2.5	54	3	6 ± 4
2.5 - 3.0	38	2	5 ± 4
3.0 - 3.5	15	0	0
3.5 - 4.0	7	1	14 ± 14
0.0 - 4.0	...	...	59 ± 17

sensitive to companion stars than Duquennoy & Mayor's (1991) survey. However, the solar-type main-sequence sample has already been corrected for undetected companion stars down to visual magnitude differences of 7.0 mag, whereas the T Tauri results are sensitive to companions with magnitude difference of at most 4.0 mag. Although it is difficult to determine how ΔK's for T Tauri stars correspond to ΔV's for main-sequence stars, it seems unlikely that the apparent overabundance of companion stars among the T Tauri stars compared to the solar-type main-sequence stars is the result of undetected companions in Duquennoy and Mayor's sample.

This T Tauri star survey is magnitude limited, which makes it possible for the binary star frequency to be artificially high if the inclusion of the companions in Table 3 in the total magnitude of the system raises them above the magnitude limit. All the observed multiple star systems have primary star K magnitudes, obtained by combining the measured flux density ratios (Table 3) with the total flux densities (Table 1), that are brighter than the magnitude limit of the survey, and therefore do not appear to be biasing the measured T Tauri binary star frequency. The magnitude limit, however, does select for the more luminous and therefore younger portion of the T Tauri star population given the vertical nature of the evolutionary tracks.

With this caveat, we assume that the difference in the binary star frequency between the T Tauri stars and their older counterparts on the main sequence is due to an intrinsic difference in their properties (i.e., the binary frequency depends on the age of the stars) and that the stars in the current T Tauri star sample will have the same properties as the solar-type main-sequence sample once they evolve down to the main sequence.

If the T Tauri stars and solar-type main-sequence stars have the same number of companion stars integrated over all possible separations, then the observed difference would be the result of a more peaked distribution for the T Tauri stars. This would imply that the distribution of binary stars as a function of separation spreads or relaxes as a function of time. However, the binary star frequency for solar-type main-sequence stars integrated over all separations is 62 [±6]%, which is comparable to the binary star frequency of T Tauri stars in the limited projected linear separation range 16 to 252 AU and leaves only 2(±11) companion stars to be found outside the separation range 16 to 252 AU if the total number of companions is to be conserved as a function of age. Tables 3 and 4 indicate that 16 compan-

TABLE 9. Overlap of sample with different surveys.

Technique	Ref	Separation Range (arcsec)	$N_{overlap}$	N_t	Triple Star $Freq_{pred}$ (%)
Direct Imaging	1,2	≥1.8 - 13	27	4	15
Lunar Occultation	1	0.005 - 0.1	16	1	6
Spectroscopy	3,4,5	0.0002 - 0.003	33	4	12
Speckle	6	.1 - 1.8	64	1	2
All	1,2,3,4,5,6	0.0002 - 13	-	-	35

Notes: $N_{overlap}$ is the number of overlap objects, i.e., the number of targets in the specified survey that are also in the complete sample of this work. N_t is the number of overlap objects that have companions observed both in the specified separation range and in the speckle imaging survey and are therefore triple or higher order systesms. The triple (or higher order) star frequency predicted is given by $\frac{N_t}{N_{overlap}} \times 100\%$. The last entry combines all the surveys to predict a triple (or higher order) star frequency of 35% for the T Tauri star sample.

(1) Simon et al. (1992)
(2) Simon (1992b)
(3) Mathieu et al. (1988)
(4) Mathieu (1992b)
(5) Edwards (1993)
(6) This work

ion stars have already been detected outside this separation range, even though the current knowledge of companion stars in the complete sample at all separations is far from complete. It therefore appears that the total number of companion stars is greater at the T Tauri stage of evolution than on the main sequence.

An overabundance of companion stars among the T Tauri stars as compared to the solar-type main-sequence star requires that some of the current T Tauri star pairs be disrupted by the time they evolve to the main sequence. The incomplete overlap of this sample with those observed with other techniques has already revealed that at least 14% of the target stars in this sample are members of systems with three or more components (see Tables 3 and 4), whereas Duquennoy & Mayor (1991) find that only 5% of their solar-type main-sequence targets are members of these higher order systems. Furthermore, the incomplete overlap of only the various surveys, as opposed to isolated observations, done with other techniques predicts that ~35% of the targets are triple or higher order systems with one component observable by speckle imaging (see Table 9). Thus one possible mechanism for reducing the number of star pairs in the separation range 16 to 252 AU with increasing age is the disruption of young triple or higher order systems. The triples and quadruples that have been observed so far are all in hierarchical systems, i.e., the ratio of separations in the system is large (≥10) and are therefore relatively stable in isolation, but could be "ionized" by close encounters with another star or system of stars. If disruption occurs, then the more widely separated stars (or pair of stars) would be more likely to break away. Thus one would expect to observe no difference between the T Tauri and the main-sequence binary star frequencies at the shortest separation. This is consistent with current spectroscopic measurements of T Tauri stars, which reveal a binary star frequency at periods less than 100 days, or equivalently at the smallest separation, that is similar to that of the solar-type main-sequence stars (Mathieu *et al.* 1988; Mathieu 1992a). Thus the discrepancy between the number of companion stars observed for the T Tauri stars and the solar-type main-sequence stars may result from the disruption of some young triple and quadruple systems before they reach the main sequence.

6. SUMMARY

We have carried out a magnitude limited ($K <= 8.5$ mag) multiplicity survey of T Tauri stars in the two nearest star forming regions the northern hemisphere, Tau–Aur and Oph–Sco. Each of the 69 stars in the sample was imaged using two-dimensional speckle interferometric techniques. On average these observations were sensitive to binary stars with magnitude differences up to 3.1 mag and separations ranging from 0".1 to 1".8. Thirty-three companion stars were found, of which nine are new detections.

There appears to be no statistically significant difference between the binary star frequency of Tau–Aur and Oph–Sco. Similarly, the binary star frequency in the high mass cloud core ρ Oph compared to that of the remainder of the sample shows no significant difference, although the small number of stars in ρ Oph renders this comparison fairly inconclusive.

There is a distinction between the classical T Tauri stars (CTTS) and the weak-lined T Tauri stars (WTTS) based on the binary star frequency as a function of separation; the WTTS binary star distribution is enhanced at the smaller separations compared to the CTTS binary star distribution. The crossover separation occurs near 100 AU, the size typically quoted for a circumstellar disk. We suggest that all T Tauri stars begin as CTTS and become WTTS when accretion has ceased and that the nearby companion stars act to shorten the accretion time scale in multiple star systems.

Integrated over all magnitude differences the binary star frequency in the projected linear separation range 16 to 252 AU for T Tauri stars (60[±17]%) is a factor of 4 greater than that of the solar-type main-sequence stars (16 [±3]%). We propose that the observed overabundance of companions to T Tauri stars with respect to their older counterparts on the main sequence is an evolutionary effect; in this scheme triple and higher order T Tauri systems, which are observed at higher frequencies than for the

solar-type main-sequence stars, are ionized by close encounters with another star or system of stars.

We thank the staff of Palomar Observatory, especially the night assistants Juan Carrasco and Will McKinley, for their assistance during the observations and J. Graham, D. McCarthy, A. Sargent, M. Simon, and B. T. Soifer for many helpful discussions. We are grateful to S. Beckwith, P. Gorham, C. Haniff, C. Koresko, and S. Kulkarni for both shared telescope time and productive interactions and we are indebted to Fred Walter who kindly provided a target list of x-ray identified sources in the Oph–Sco regions prior to publication as well as many helpful comments in reviewing this paper. Tom Prince and the Caltech Conconcurrent Supercomputing Facility generously provided time on the Caltech NCUBE supercomputer for the speckle imaging data reduction. This research has made use of the SIMBAD data base, operated at CDS, Strasbourg, France. Infrared astrophysics at Caltech is supported by a grant from the NSF. A. G. currently receives support from NASA through Grant No. HF-1031.01-92A awarded by the Space Telescope Science Institute which is operated by the Association of Universities for Research in Astronomy, Inc., for NASA under Contract No. NAS5-26555.

APPENDIX: THE BINARY STAR FREQUENCY OF MAIN-SEQUENCE STARS

Duquennoy & Mayor (1991) searched a total of 164 nearby solar-type main-sequence stars for companion stars and found that the number of companion stars as a function of the orbital period, P, could be fit by a Gaussian distribution in $\log P$. Figure 14(a) reproduces their binned, bias-corrected data as well as their model fit. To compare this work to the T Tauri star sample, their distribution is converted to a function of average projected linear separation ($\langle a \rangle$). The period is converted to its corresponding semimajor axis, A, using Kepler's law and assuming an average primary star mass of $1\mathcal{M}_{\odot}$ and an average mass ratio between the components of 0.40 (from Duquennoy and Mayor's Fig. 10). The semimajor axis is translated to an average projected separation based on a Monte-Carlo simulation carried out by Fischer & Marcy (1992), which givers the following relationship,

$$A = 1.26\langle a \rangle.$$

The distribution of solar-type main-sequence star companion stars as a function of $\langle a \rangle$ is then rebinned, using Duquennoy and Mayor's model fit. Figure 14(b) shows the result of rebinning the main-sequence data, such that the new bin width matches the separation range $\Delta \log \langle a \rangle_{AU} = 1.2$, and normalizing the distribution by the total number of target stars (164) to produce a binary star frequency distribution. Integrated over the projected linear separation range 16 to 252 AU, the binary star frequency of nearby solar-type main-sequence stars is 16[±3]%, where the uncertainty is based on Poisson statistics.

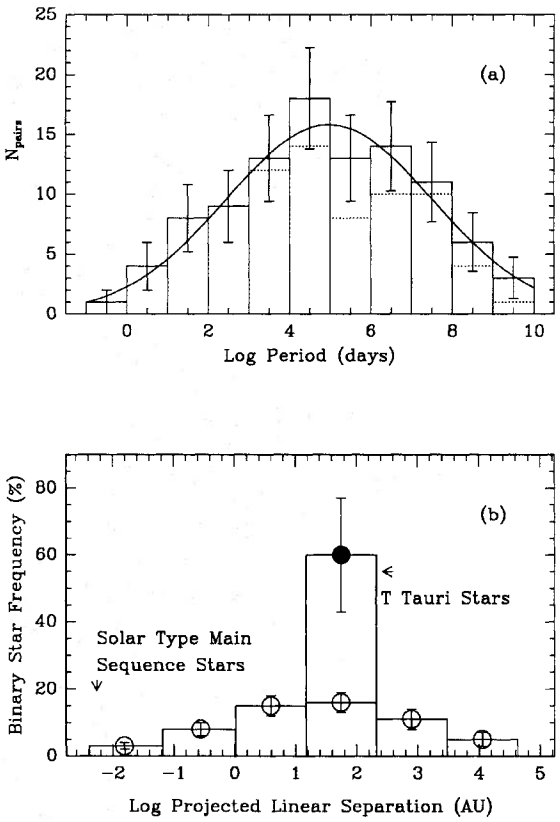

FIG. 14. (a) The distribution of companion stars in the nearby sample of solar-type main-sequence stars as a function of orbital period, taken from Duquennoy & Mayor (1991) (b) The hatched histogram is the binary star frequency of the solar-type main-sequence stars as a function of average projected linear separation. Also shown is the binary star frequency of the T Tauri stars (the unhatched region). The Tauri binary star frequency appears to be a factor of 4 greater than that of the solar-type main-sequence stars.

Fischer & Marcy (1992) compile the results of several M dwarf surveys, conducted with different observing techniques, to determine the multiplicity of these low mass main-sequence stars. They quote their results in terms of the number of companion stars per target per AU for a given range of semimajor axes (their Table 2). Based on their relationship between $\langle a \rangle$ and A to convert these binary star frequencies to a function of $\langle a \rangle$ and an integration of these values over 16 to 252 AU, the binary star frequency in this range for the M dwarfs is estimated to be 12[±4]%.

REFERENCES

Abt, H. A. 1983, ARA&A, 21, 343
Abt, H. A., & Levy, S. G 1976, ApJSS, 30, 273
Adams, F. C., Lada, C. J., & Shu, F. H. 1988, ApJ, 326, 865
Aitken, R. F. 1932, in A New General Catalog of Double Stars Within

120° of the North Pole (Carnegie Institution, Washington, D.C.)
Basri, G., & Batalha, C. 1990, ApJ, 363, 654
Basri, G., & Bertout, C. 1989, ApJ, 341, 340
Beckwith, S. V. W., & Sargent, A. I. 1992, in Protostars and Planets III, edited by E. H. Levy and J. Lunine, preprint
Beckwith, S. V. W., Sargent, A. I., Chini, R. S., & Gusten, R. 1990, AJ, 99, 924
Blaauw, A. 1964, ARA&A, 2, 213
Bouvier, J., & Appenzeller, I. 1991, A&ASS, 92, 481
Bouvier, J., Tessier, E., & Cabrit, S. 1992, A&A, preprint
Cabrit, S., Edwards, S., Strom, S. E., & Strom, K. M. 1990, ApJ, 354, 687
Chelli, A., Zinnecker, H., Carrasco, L., Cruz-Gonzalez, I., & Perrier, C. 1988, A&A, 207, 46
Chen, W. P., Simon, M., Longmore, A. J., Howell, R. R., & Benson, J. A. 1990, ApJ, 357, 224
Christou, J. C., Cheng, A. Y. S., Hege, K. E., & Roddier, C. 1985, AJ, 90, 2644
Cohen, M., Emerson, J. P., & Beichman, C. A. 1989, ApJ, 339, 455
Cohen, M., & Kuhi, L. V. 1979, ApJSS, 41, 743
de Geus, E. J., de Zeeuw, P. T., & Lub, J. 1989, A&A, 216, 44
de Geus, E. J., Bronfman, L., & Thaddeus, P. 1990, A&A, 231, 137
de Geus, E. J., & Burton, W. B. 1991, A&A, 246, 559
Duquennoy, A., & Mayor, M. 1991, A&A, 248, 485
Dyck, H. M., Simon, T., & Zuckerman, B. 1982, ApJ, 255, L103
Edwards, S. 1993, private communication
Elias, J. H. 1978, ApJ, 224, 857
Fischer, D. A., & March, G. W. 1992, ApJ, 396, 178
Ghez, A. M. 1992, Ph.D. thesis, California Institute of Technology
Ghez, A. M., Neugebauer, G., Gorham, P. W., Haniff, C. A., Kulkarni, S. R., Matthews, K., Koresko, C., & Beckwith, S. 1991, AJ, 102, 2066
Glass, I. S., & Penston, M. V. 1974, MNRAS, 167, 237
Gorham, P. W., Ghez, A. M., Haniff, C. A., & Prince, T. A. 1990, AJ, 100, 294
Graham, J. 1991, private communication
Haas, M., Leinert, Ch., & Zinnecker, H. 1990, A&A, 230, L1
Haro, G., & Chavira, E. 1974, Inf. Bull. Var. Stars, 926
Hartigan, P., Kenyon, S. J., Hartmann, L., Strom, S. E., Edwards, S., Welty, A. D., & Stauffer, J. 1991, ApJ, 382, 617
Heintz, W. D. 1980, ApJSS, 44, 111
Henry, T. J. 1991, Ph.D. thesis, University of Arizona
Henry, T. J., McCarthy, D. W., Freeman, J., & Christou, J. C. 1992, AJ, 103, 1369
Herbig, G. H. 1977, ApJ, 214, 747
Herbig, G. H., & Bell, K. R. 1988, Lick Obs. Bull. No. 1111
Herbig, G. H., Vrba, F. J., & Rydgren, A. E. 1986, AJ, 91, 575
Herbst, W., & Warner, J. W. 1981, AJ, 86, 885
Joy, A. H., & Van Biesbroeck, G. 1944, PASP, 56, 123
Koresko, C. D., Beckwith, S. V. W., Ghez, A. M., Matthews, K., & Neugebauer, G. 1991, AJ, 102, 2073
Lada, E. A., Strom, K. M., & Myers, P. C. 1992, in Protostars and Planets III, edited by E. H. Levy and J. Lunine, preprint
Leinert, Ch., Haas, M., Richichi, A., Zinnecker, H., & Mundt, R. 1991, A&A, 250, 407
Leinert, Ch., *et al.* 1992, Complementary Approaches to Double and Multiple Star Research, IAU Colloquium No. 135, edited by H. A. McAlister and W. I. Hartkopf (ASP, San Francisco), p. 21
Lin, D. N. C., & Papaloizou, J. C. B 1992, in Protostars and Planets III, edited by E. H. Levy and J. Lunine, preprint
Lynds, B. T. 1962, ApJSS, 7, 1
Mathieu, R. D., Walter, F. M., & Myers, P. C. 1988, AJ, 98, 987
Mathieu, R. D. 1992a, Complementary Approaches to Double and Multiple Star Research, IAU Colloquium No. 135, edited by H. A. McAlister and W. I. Hartkopf (ASP, San Francisco), p. 30
Mathieu, R. D. 1992b, private communication
McAlister, H. A., & Hartkopf, W. I. 1988, Second Catalog of Interferometric Measurements of Binary Stars (Center for High Angular Resolution Astronomy)
Moneti, A., & Zinnecker, H. 1991, A & A, 242, 428
Montmerle, T., Koch-Miramond, L., Falgarone, E., & Grindlay, J. E. 1983, ApJ, 269, 182
Myers, P. C. 1985, in Protostars and Planets II, edited by D. C. Black and M. S. Mathews, p. 81
Rydgren, A. E., Schmelz, J. T., & Vrba, F. J. 1982, ApJ, 256, 168
Rydgren, A. E., Strom, S. E., & Strom, K. M. 1976, ApJSS, 30, 307
Rydgren, A. E., & Vrba, F. J. 1981, AJ, 86, 1069
Rydgren, A. E., & Vrba, F. J. 1983, AJ, 88, 1017
Shu, F. H., Adams, F. C., & Lizano, S. 1987, ARA&A, 25, 23
Simon, M. 1992a, Complementary Approaches to Double and Multiple Star Research, IAU Colloquium No. 135, edited by H. A. McAlister and W. I. Hartkopf (ASP, San Francisco), p. 41
Simon, M. 1992b, private communication
Simon, M., Chen, W. P., Howell, R. R., Benson, J. A., & Slowik, D. 1992, ApJ, 384, 212
Simon, M., Howell, R. R., Longmore, A. J., Wilking, B. A., Peterson, D. M., & Chen, W. P. 1987, ApJ, 320, 344
Skrutskie, M. F. 1992, private communication
Strom, K. M., Strom, S. E., Edwards, S., Cabrit, S., & Skrutskie, M. F. 1989, AJ, 97, 1451
Ungerechts, H., & Thaddeus, P. 1987, ApJSS, 63, 645
Walter, F. M. 1986, ApJ, 306, 573
Walter, F. M., Brown, A., Mathieu, R. D., Myers, P. C., & Vrba, F. J. 1988, AJ, 96, 297
Walter, F. M., Vrba, F. J., Mathieu, R. D., Brown, A., & Myers, P. C. 1993, in preparation
Warner, G., Strom, S. E., & Strom, K. M. 1977, ApJ, 213, 427
Weintraub, D. 1989, Ph.D. thesis, University of California, Los Angeles
Wilking, B. A., & Lada, C. J. 1983, ApJ, 274, 698
Wilking, B. A., Lada, C. J., & Young, E. T. 1989, ApJ, 340, 823
Zinnecker, H., Brandner, W., Reipurth, B. 1992, Complementary Approaches to Double and Multiple Star Research, IAU Colloquium No. 135, edited by H. A. McAlister and W. I. Hartkopf (ASP, San Francisco), p. 50